

Multipolar nonlinear nanophotonics

Daria Smirnova and Yuri S. Kivshar*

Nonlinear Physics Centre, Australian National University, Canberra ACT 2601, Australia

(Dated: August 3, 2016)

Nonlinear nanophotonics is a rapidly developing field with many useful applications for a design of nonlinear nanoantennas, light sources, nanolasers, sensors, and ultrafast miniature metadevices. A tight confinement of the local electromagnetic fields in resonant photonic nanostructures can boost nonlinear optical effects, thus offering versatile opportunities for subwavelength control of light. To achieve the desired functionalities, it is essential to gain flexible control over the near- and far-field properties of nanostructures. Thus, both modal and multipolar analyses are widely exploited for engineering nonlinear scattering from resonant nanoscale elements, in particular for enhancing the near-field interaction, tailoring the far-field multipolar interference, and optimization of the radiation directionality. Here, we review the recent advances in this recently emerged research field ranging from metallic structures exhibiting localized plasmonic resonances to hybrid metal-dielectric and all-dielectric nanostructures driven by Mie-type multipolar resonances and optically-induced magnetic response.

INTRODUCTION

Modern nanophotonics aims toward the efficient light manipulation at the nanoscale and the design of ultrafast compact optical devices for fully-functional photonic circuitry integrable with the state-of-art nanoscale electronics [1–6]. Within decades of fruitful developments, nanophotonics has become a prominent area of research with applications ranging from the high-performance data processing and optical computing to super-imaging and biosensing [7–12]. Many branches of nanophotonics commonly rely on strong light-matter interaction in the resonant subwavelength structures due to the enhanced near fields [13], achieved through the excitation of trapped electromagnetic modes, sustained by the nanoelements, or localized geometrical resonances [14]. Resonant tight field confinement is indispensable particularly for the efficient intensity-dependent effects with practically important nonlinear optical applications, such as frequency conversion, wave-mixing, Raman scattering, self-action, and all-optical switching. While in bulk macroscopic media efficiencies of nonlinear optical phenomena are largely determined by the intrinsic nonlinear properties and phase-matching requirements [15], efficiencies of nonlinear processes and effective susceptibilities, which may be assigned to nanostructured materials to characterize their nonlinear response, can be significantly increased through enhanced local fields at resonances. Therefore, nonlinear response significantly depends on localized resonant effects in nanostructures, allowing for nonlinear optical components to be scaled down in size and offering exclusive prospects for engineering fast and strong optical nonlinearity and all-optical light control at the nanoscale.

The present-day nanophotonics has greatly advanced in the manufacturing and study of open nanosize optical resonators that are actually resonant *nanoantennas*,

which couple localized electromagnetic field and freely propagating radiation [16, 17]. Metal nanoparticles [14] sustaining surface plasmon-polariton modes as well as dielectric counterparts with high enough index of refraction [18, 19] are utilized as such resonators, and serve for applications in nonlinear diagnostics and microscopy. In turn, two- and three-dimensional clusters and regular arrays of such nanoparticles, employed as unit cells, resonantly responding to IR radiation and visible light, constitute optical metasurfaces and metamaterials (artificial media with pre-designed properties) by analogy with microwave systems [20–22].

Multipole decomposition. Generally, in the problems of both linear and nonlinear scattering at arbitrary nanoscale objects, multipole decomposition of the scattered electromagnetic fields provides a transparent interpretation for the measurable far-field characteristics, such as radiation efficiency and radiation patterns, since they are essentially determined by the interference of dominating excited multipole modes [23–30].

In terms of the electric a_E and magnetic a_M scattering coefficients, the total time-averaged scattered power (energy flow) is given by

$$W_s = \frac{\pi |E_0|^2}{2\eta k^2} \sum_{l=1}^{\infty} \sum_{m=-l}^l (2l+1) (|a_E(l, m)|^2 + |a_M(l, m)|^2), \quad (1)$$

revealing the input of each multipolar excitation (namely, dipole at $l = 1$, quadrupole at $l = 2$, octupole at $l = 3$, etc). Here, $k = \omega \sqrt{\varepsilon \mu}$ is the wavenumber in the medium, $\eta = \sqrt{\mu/\varepsilon}$ is the impedance, E_0 is an electric field amplitude, l and m are angular momentum (orbital) and magnetic quantum numbers, respectively. Equation (1) is written in SI units under the normalization accepted in Ref. [30]. To describe the radiation from arbitrary localized sources, the multipole coefficients $a_{E,M}$ can be retrieved either through the volume integration of the source current density distribution, or by taking angular integrals of radial (or angular) components of the numerically pre-calculated electromagnetic fields with spherical

* Corresponding author: ysk@internode.on.net

harmonics over a spherical surface enclosing a scatterer. If no analytical solution can be obtained, the field at the surface of such a sphere can be found with the use of numerical codes or modern commercial full-wave solvers.

Assuming the far-field asymptotic of the outgoing spherical wave, the field expansion into the vector spherical harmonics $\mathbf{X}_{l,m}(\theta, \phi)$ recovers the directional dependence of the radiation,

$$\frac{dP(\theta, \varphi)}{d\Omega} = \frac{\pi|E_0|^2}{2\eta k^2} \left| \sum_{l=1}^{\infty} \sum_{m=-l}^l (-i)^{l+1} (2l+1) \cdot (i^l a_M(l, m) \mathbf{X}_{l,m} + i^{l+1} a_E(l, m) \hat{\mathbf{r}} \times \mathbf{X}_{l,m}) \right|^2, \quad (2)$$

defined as a power per unit solid angle Ω in spherical coordinates $\{\theta, \varphi\}$, $\hat{\mathbf{r}}$ denotes the unit radius vector. The scattered electric far-field can also be conveniently expressed through the decomposition in the Cartesian multipolar terms [23] as a sum

$$\mathbf{E}_{\text{sca}} = \mathbf{E}_{\text{ED}} + \mathbf{E}_{\text{MD}} + \mathbf{E}_{\text{EQ}} + \dots = \frac{k^2}{4\pi\epsilon_0} \frac{e^{ikr}}{r} \left\{ [(\hat{\mathbf{r}} \times \mathbf{p}) \times \hat{\mathbf{r}} - \frac{1}{c} \hat{\mathbf{r}} \times \mathbf{m} - \frac{ik}{6} [(\hat{\mathbf{r}} \times \mathbf{Q}(\hat{\mathbf{r}})) \times \hat{\mathbf{r}}] + \dots \right\}, \quad (3)$$

where \mathbf{p} , \mathbf{m} and \mathbf{Q} are the electric dipole (ED), magnetic dipole (MD) and electric quadrupole (EQ) leading moments, respectively, and ϵ_0 is the vacuum permittivity. Tuning the contributions of different-order multipole moments is used to engineer the scattering and tailor the emission directionality of optical nanoantennas [18, 31–39]. In particular, the so-called first Kerker condition for overlapped and balanced orthogonal electric and magnetic dipoles represents an example of *unidirectional scattering* [40] from a single-element antennas. The scattering is interferentially suppressed in either backward or forward (z) direction, if the relation $1/\epsilon_0 p_x = \pm \eta m_y$ holds for the only non-negligible Cartesian electric p_x and magnetic m_y dipolar moments induced in a particle along the x and y axes, respectively. Developing this concept, the directionality of the scattering can be improved through the interference of properly excited higher-order electric and magnetic modes [41–44].

However, the local-field features and far-field properties are intimately linked in the nonlinear response of nanostructures [45, 46]. A formal way to quantify this effect is based on the Lorentz reciprocity theorem. In particular, this method allows one to predict the metamaterial nonlinearity by using linear calculations [46], and to express the excitation coefficients of spherical multipoles, the radiated field is decomposed into, through the overlap integrals of the nonlinear source and the respective spherical modes [47]. In this regard, two key ingredients to realize strong nonlinear response from nanostructures are usually emphasized: the local field enhancement and

modal overlaps. For instance, the efficiency of harmonic generation can be strongly enhanced in nanostructures, provided the pump or generated frequency matches the supported resonance [15], especially, if the geometry is doubly resonant [48–52], i.e. it sustains resonances at both the fundamental and harmonic frequencies, and spatial distribution of the nonlinear source is such that it strongly couples the corresponding modes.

For metamaterials, the applicability of simple estimates based on the nonlinear oscillator model [53, 54] and Miller’s law [55, 56] is limited to the specific cases only [46, 57], e.g. odd in frequency third-harmonic generation [58–60]. In fact, the character and efficiency of the nonlinear response in nanostructures are highly affected by many factors [61], including variations in their size, shape, material filling fractions, quality of samples, interparticle interactions, spatial symmetries of both geometry and excitation beams [62], linear scattering properties. Nonetheless, to a large extent, the key governing features may be approached with the analysis of the unique resonant behaviour of these artificial materials [63], as well as strengths and mutual interference of the leading excited or generated field multipoles [64].

Nonlinear response. Within the macroscopic description utilizing Maxwell’s equations, nonlinear optics employs the nonlinear constitutive relations. For example, in the electric dipole approximation of light-matter interaction, the material response in a nonmagnetic medium can be specified by the nonlinear relationship between the applied electric field \mathbf{E} and induced polarization \mathbf{P} as

$$\mathbf{P} = \epsilon_0 \left[\overset{\leftrightarrow}{\chi}^{(1)} \cdot \mathbf{E} + \overset{\leftrightarrow}{\chi}^{(2)} : \mathbf{E}\mathbf{E} + \overset{\leftrightarrow}{\chi}^{(3)} : \mathbf{E}\mathbf{E}\mathbf{E} + \dots \right], \quad (4)$$

written in the form of an asymptotic expansion in a Taylor series. Here, the first term corresponds to the linear regime at weak excitation fields, and $\overset{\leftrightarrow}{\chi}^{(N)}$ are the N -th order susceptibility tensors of rank $N+1$, which capture both the polarization dependent nature of the parametric interaction as well as the symmetries of the specific material. Since the optical nonlinearities of natural materials are rather weak, the nonlinear scattering manifests itself at sufficiently strong applied electromagnetic fields, achievable with powerful coherent light sources. Given the fact that considerable amounts of electromagnetic energy can be confined to tiny volumes in nanoparticles or even smaller hot spots, they enable downscaling the required optical powers, because the intensity of SHG/THG processes scales with the fourth/sixth power of the fundamental field strength.

Symmetry considerations appear to be of particular importance in nonlinear optics. For instance, the second-order nonlinear effects are inhibited in the bulk of such uniform centrosymmetric media, such as plasmonic metals and group IV semiconductors, within the electric dipole approximation of the light-matter interaction because of the symmetry constraints, while no such restriction exists for third-order processes [65]. However,

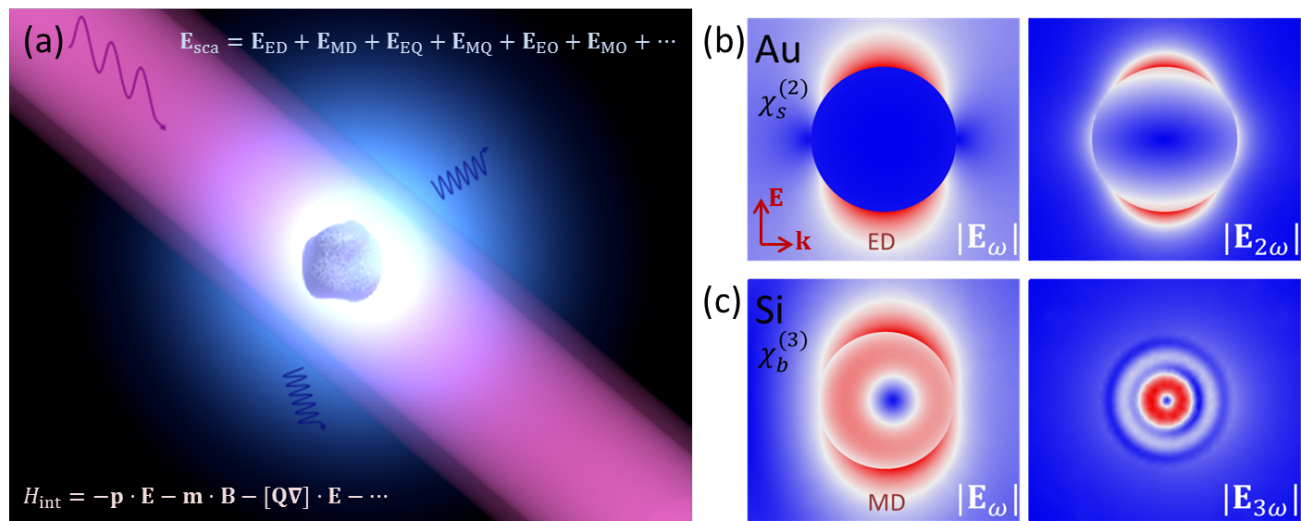


Figure 1. (a) Schematic of nonlinear light scattering by an arbitrarily shaped nanoparticle. The formulae delineate the light-matter interaction Hamiltonian (bottom) and the nonlinearly generated field (top) expanded in terms of multipole moments. Illustrations of (b) SHG and (c) THG from a single spherical nanoparticle made of gold and silicon, respectively. Shown are near-field distributions of the electric field magnitude at the fundamental and harmonic frequencies. Nonlinear response of a 150 (600) nm diameter gold (silicon) nanoparticle is driven by ED (MD) mode at wavelength $\lambda_0 = 0.794$ (2.15) μm and dominated by the surface (bulk) nonlinear polarization source, characterized by the nonlinear susceptibility tensor $\chi_s^{(2)}$ ($\chi_b^{(3)}$) of the second (third) order. Polarization of the exciting plane wave is specified by red arrows in caption (b).

the inversion symmetry is broken at interfaces, thus enabling the second-order nonlinear processes from surfaces of isotropic crystals due to the electric-dipole surface contribution to the nonlinear polarization. Its sensitivity to surface properties is used in probing techniques. The bulk nonlinear polarization arises from higher-order nonlocal magnetic-dipole and electric-quadrupole interactions with light at the microscopic level. To account for the multipolar orders, the effective light-matter interaction Hamiltonian [1, 66] is expanded as such

$$H_{\text{int}} = -\mathbf{p} \cdot \mathbf{E} - \mathbf{m} \cdot \mathbf{B} - [\mathbf{Q}\nabla] \cdot \mathbf{E} - \dots, \quad (5)$$

where the electric dipole \mathbf{p} , magnetic dipole \mathbf{m} and electric quadrupole moments \mathbf{Q} are here interpreted as operators.

The aim of this review paper is twofold. First, within the connecting frame of multipolar scattering, we discuss the nonlinear optical effects at the nanoscale. Importantly, the physics of supported resonances and material properties in plasmonic and dielectric nanoparticles are different, as illustrated in Fig. 1, and therefore we consider metallic, metal-dielectric and all-dielectric structures separately. Second, we emphasize the importance of the optically-induced magnetic resonances in hybrid and high-index dielectric nanostructures which may lead to a substantial enhancement of the nonlinear response and novel ways to control directionality of the nonlinear radiation.

PLASMONIC NANOPARTICLES

To date, the possibilities of nanoscale confinement of light are primarily associated with plasmon-polaritons, which are collective excitations originating from coupling of the electromagnetic fields to electron oscillations in a metal plasma [7]. Physics of light interaction with metal structures that are much smaller than the free space wavelength of light constitutes one of the most significant branches of contemporary nanophotonics *nanoplasmonics*. Combining strong localized surface plasmon resonances and high intrinsic nonlinearities, plasmonic structures offer a unique playground to study a rich diversity of nonlinear phenomena, including second-harmonic generation (SHG) [8, 67–71], third-harmonic generation (THG) [58–60, 65], four-wave mixing (FWM) [72], multiphoton luminescence [73], self-action effects [74–78]. In a broader scope, the intense electric near-fields may also boost (enhance) the nonlinear response in the materials brought into the proximity of plasmonic nanoantennas [79–84]. Some important aspects of *nonlinear plasmonics* were reflected in several recent review papers [68–70, 85].

Plasmons are commonly associated with conventional metals (gold, silver, copper and aluminum) possessing a large number of quasi-free conduction electrons which oscillate collectively in response to the applied harmonic field. *Electric dipolar resonance* caused by such plasma oscillations in finite structures is most widely exploited for small metallic particles and their composites in nonlinear plasmonics [58–60, 68]. Noticeably, for deep sub-

wavelength scatterers, even when the excitation wavelength is strongly detuned from the resonance frequency, the electric dipole order dominates over the higher-order excitations in the multipolar decomposition.

The bulk of plasmonic metals formed by atoms organized in face-centered cubic lattices exhibits a center of symmetry. Assuming a particle made of a centrosymmetric isotropic homogeneous medium, the SH polarization source can be written as a sum of nonlocal-bulk and local-surface contributions,

$$\mathbf{P}^{(2\omega)} = \mathbf{P}_{\text{surf}}^{(2\omega)} + \mathbf{P}_{\text{bulk}}^{(2\omega)}, \quad (6)$$

$$\mathbf{P}_{\text{surf}}^{(2\omega)} = \varepsilon_0 \overset{\leftrightarrow}{\chi}_s^{(2)} : \mathbf{E}^{(\omega)} \mathbf{E}^{(\omega)} \delta(\mathbf{r} - \mathbf{r}_s) \equiv \mathbf{P}_s^{(2\omega)} \delta(\mathbf{r} - \mathbf{r}_s), \quad (7)$$

$$\mathbf{P}_{\text{bulk}}^{(2\omega)} = \varepsilon_0 \overset{\leftrightarrow}{\chi}_b^{(2)} : \mathbf{E}^{(\omega)} \nabla \mathbf{E}^{(\omega)}, \quad (8)$$

where \mathbf{r}_s defines the surface, $\overset{\leftrightarrow}{\chi}_s^{(2)}$ and $\overset{\leftrightarrow}{\chi}_b^{(2)}$ are the second-order susceptibility tensors. If the particle surface possesses isotropic symmetry with a mirror plane perpendicular to it, the surface second-order susceptibility tensor $\overset{\leftrightarrow}{\chi}_s^{(2)}$ has only three non-vanishing and independent elements, $\chi_{\perp\perp\perp}^{(2)}$, $\chi_{\perp\parallel\parallel}^{(2)}$ and $\chi_{\parallel\parallel\perp}^{(2)} = \chi_{\parallel\perp\parallel}^{(2)}$, where the symbols \perp (or \parallel) refer to the directions normal (tangential) to the surface [86] and, therefore, the surface polarization is recast to

$$\mathbf{P}_s^{(2\omega)} = \hat{\mathbf{n}}(\chi_{\perp\perp\perp}^{(2)} E'_n E'_n + \chi_{\perp\parallel\parallel}^{(2)} \mathbf{E}'_\tau \mathbf{E}'_\tau) + 2\chi_{\parallel\perp\parallel}^{(2)} E'_n \mathbf{E}'_\tau, \quad (9)$$

where $\mathbf{E}^{(\omega)}$ is the driving field near the interface, n and τ refer to the normal and tangent components, respectively. The bulk polarization depends on the spatial derivatives (gradients) of the electromagnetic field

$$\mathbf{P}_{\text{bulk}}^{(2\omega)} = \beta \mathbf{E}^{(\omega)} \nabla \cdot \mathbf{E}^{(\omega)} + \gamma \nabla \left(\mathbf{E}^{(\omega)} \cdot \mathbf{E}^{(\omega)} \right) + \delta' \left(\mathbf{E}^{(\omega)} \cdot \nabla \right) \mathbf{E}^{(\omega)}, \quad (10)$$

where β , γ and δ' are material parameters [25, 86]. In the homogeneous media, the first term vanishes. The component $\chi_{\perp\perp\perp}^{(2)}$ of the surface susceptibility tensor commonly yields the largest contribution to the surface SH response for metal nanoparticles [87, 88] and reaches the values of $\sim 10^{-18} \text{ m}^2 \text{V}^{-1}$ [89]. Aside from phenomenology, relying on experimental retrieval of nonlinear susceptibilities, analytical expressions for parameteres, shedding light on the origin of complex electronic nonlinearity in metals, can be derived within free-electron, hydrodynamic and quantum density functional theories [90–93]. A more involved self-consistent nonperturbative description of harmonic generation in metallic nanostructures was recently developed through transient implementation of the hydrodynamic model [94, 95].

To describe the nonlinear scattering theoretically, the nonlinear Mie theory was developed over recent

decades [29, 68, 98–103] as an extension of the analytical approach outlined in Refs. [25, 104] for the Rayleigh limit of SHG from a spherical particle. This theory can be used for particles of any sizes and materials, however being limited to strictly spherical shapes, and it is widely exploited to examine SHG governed by the dominant surface SH polarization source [87, 88] in spheroidal metallic nanoparticles. In contrast, another technique, the nonlinear Rayleigh-Gans-Debye model is applicable for particles of any shapes as long as a refractive index mismatch between the particle and a host medium is low. However, the latter is not the case for metallic particles immersed in aqueous medium, frequently employed in experiments. Numerical studies in nonlinear nanophotonics [105–107] are most commonly performed with the use of finite-element [57, 108–110] method, integral equation techniques [111–113], hydrodynamic models [92, 94] and FDTD [114].

In the small-particle limit $kR \ll 1$, it was proven analytically that nonlinear local electric quadrupole and nonlocal electric dipole, originating from the retardation effect, excited in a spherical metal nanoparticle of radius R at the SH frequency provide the main contributions to the SHG radiation [25, 104], whereas the linear scattering properties of small particles are largely determined by the electric dipolar response. This deduction has been also supported by extensive experimental studies [110, 115, 116]. Deformation effects, causing the deviation of the particle shape from a perfect sphere, allow for the SH emission from the locally excited dipole [117, 118]. With increasing the particle size, the onset of an octupolar contribution was detected for Au nanoparticles of 70 nm in diameter [88, 109].

Figure 2(a) demonstrates the angle-resolved second-harmonic scattering (AR-SHS) pattern from 80 nm diameter Ag nanoparticles in water excited at the fundamental wavelength 800 nm [96]. In agreement with theoretical predictions, the dominant surface susceptibility component $\chi_{\perp\perp\perp}^{(2)}$ drives a quadrupolar-like SH emission. For comparison, AR-SHS pattern from nonplasmonic similarly-sized spherical polystyrene nanoparticles adsorbed with nonlinear-optically active malachite green molecules (MG/PS) (88 nm diameter) excited at 840 nm is shown in the inset. In the latter case, nonlocally excited dipole emission characterized by two lobes stems from the different leading component $\chi_{\perp\parallel\parallel}^{(2)}$.

Spectral and angular properties of SHG from plasmonic nanoparticles are largely influenced by structural symmetries of both scatterer and external field, a type of excitation [119, 120], spatial variations of the applied electromagnetic field and field gradients at nanoscale, and it can be significantly enhanced in the vicinity of plasmonic resonances known for their inherent geometric tunability. For instance, synthetic nonlinear media can be designed from reduced-symmetry 3D plasmonic elements, such as nanocups consisting of a spherical metal semishell fabricated around a dielectric nanoparticle core [97]. Symmetry breaking in this geometry intro-

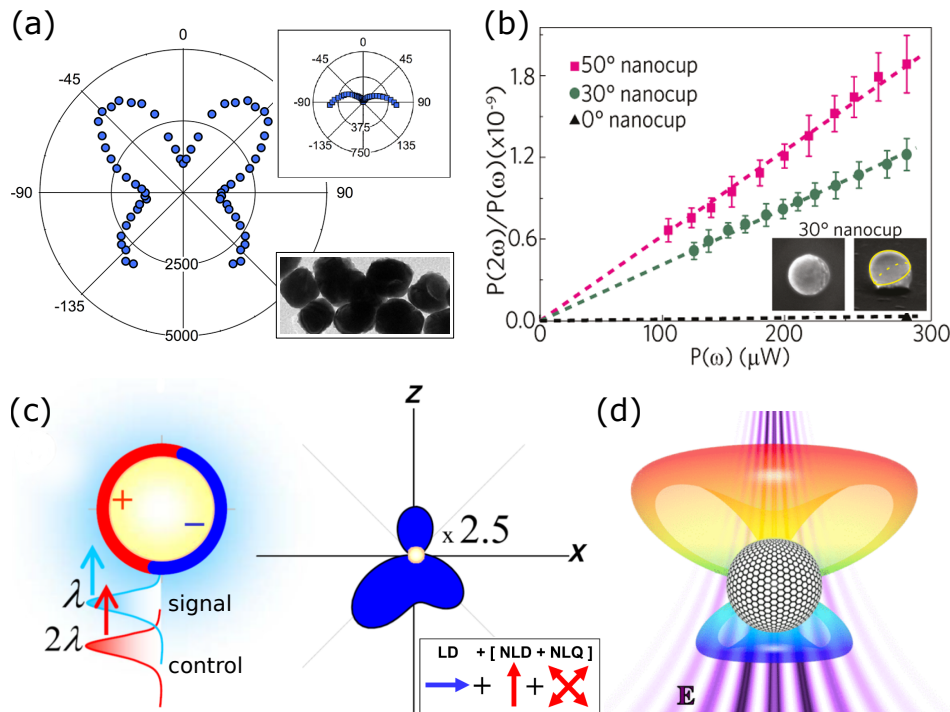


Figure 2. (a) SH scattering pattern from Ag nanoparticles in water with four well-resolved quadrupolar lobes. Inset: SH scattering pattern from MG/PS nanoparticles featuring a dominant nonlocally excited electric dipole (top); TEM image of Ag nanoparticles (bottom). (b) SH conversion efficiency by individual nanocup scales linearly as a function of the incident laser power and increases with nanocup angle. Inset: SEM image of a chemically synthesized nanocup on a glass substrate oriented at 30° to the substrate normal. 120 nm silica nanoparticle is capped with a 35nm-thick Au layer. (c) Coherent control of light scattering from a gold nanowire by two collinear signal and control beams with zero phase delay. (d) Schematic view of a graphene-wrapped nanoparticle placed into an axially symmetric slightly inhomogeneous external field. The SH radiation predominantly directed into the upper half-space. Panels (a-d) are adopted from Refs. [96], [97], [32], [36], respectively.

duces a magnetic dipole mode, when a nanocup resembles a resonant LC circuit. Both intensity and emission profiles of the enhanced SHG from such a nanocup excited at the magnetic dipole resonance were observed to depend on a nanocup orientation. The conversion efficiency increases dramatically as the angle between the pump excitation direction and the nanocup symmetry axis is increased, as shown in Fig. 2(b), while the scattering directionality is dictated by a nanocup inclination, regardless of the excitation direction or polarization.

In the context of plasmonic nanoantennas, the idea of all-optical control of the radiation directionality through an interplay between linear scattering and second-harmonic generation was proposed in Ref. [32]. In the proof-of-concept theoretical model, the authors consider a 100 nm gold nanowire simultaneously excited by a low-intensity (signal) and high-intensity (control) fields at wavelengths $\lambda = 532$ nm and 2λ , respectively. Asymmetric scattering pattern occurs owing to the interference between the linear electric dipole (LD) induced by the signal and nonlinear dipole (NLD) and quadrupoles (NLQ) generated by the control, as exemplified in Fig. 2(c). Altering excitation conditions, the authors demonstrate that light scattering from a single nanoelement can be efficiently tuned by changing phase delay and relative angle

between two excitation beams. Similarly, in Ref. [121] it was shown that THG signal emitted from a three-nanorod gold structure can be coherently controlled by changing a relative phase of two different excitation channels. Localized surface plasmon polaritons in the nanorods are excited through near- and far-field couplings to two orthogonally polarized light fields. The cancellation of the excitation was measured as a minimum of the THG signal, and the observed phase shift between the THG signal and excitation was attributed to damping effects.

Graphene, a single atomic layer of graphite, has emerged recently as a promising alternative to noble metals for applications in plasmonics [122, 123]. The study of plasmonic effects in doped graphene structures has attracted a special interest from the nanoplasmonics research community due to novel functionalities suggested by such systems, including an extraordinary field confinement by a graphene layer, tunability of graphene properties through doping or electrostatic gating and longer lifetimes in the infrared and terahertz frequency ranges [124]. In addition, graphene demonstrates strong and tunable optical nonlinearity and it can be incorporated into various components of nanoscale optics [125–127]. The study of the nonlinear response of graphene in

the resonant plasmonic geometries is still in its infancy and is expected to bring new concepts and find real applications. Remarkably, graphene is not only employed for planar geometries, but there are also attempts to wrap complex three dimensional objects in graphene [128–130]. In Ref. [36], a theoretical model for the resonant second-harmonic generation from a graphene-wrapped dielectric spherical nanoparticle has been developed. Strong nonlinear response is caused by an induced quadratic surface current in graphene. When the particle is illuminated by a plane wave, the resonantly enhanced radiation of the second harmonic is quadrupolar and symmetric, however, the radiation pattern of the second harmonic can be manipulated by placing the particle in a weakly inhomogeneous external field, which is schematically shown in Fig. 2(d). This resultant asymmetric emission is determined by the interference of dipole and quadrupole modes and the asymmetry of the external field changes the efficiency of the excitation of these modes. For the typical parameters, the second harmonic is predominantly radiated in the halfspace with stronger external electric field.

A macroscopic description of the nonlinear response from arrays of noncentrosymmetric nanoparticles is based on the effective multipolar tensors [131–134]. In particular, the magnetic dipole and electric quadrupole contributions were experimentally identified in the nonlinear emission of L-shape gold nanoparticles through asymmetry of the generated SH field intensity measured in transmission and reflection [135]. The second-order nonlinear response of arrays of metal nanostructures and the relative importance of such multipolar effects are generally affected by the symmetry properties and shapes of scatterers, quality of samples, plasmonic enhancement and small-scale inhomogeneities of the local field, hot spots, particle arrangement and interparticle coupling [136–139].

Being the simplest nonlinear optical process, SHG was intensively studied in various plasmonic structures of different shapes and coupling [137, 139–143], chiral [144–146] and Fano-resonant geometries [147, 148]. Based on near- and far-field radiation properties, specific designs have been suggested for applications in sensing [102, 149], shape characterization [150], nonlinear nanorulers [151, 152] and nonlinear microscopy [153].

METAL-DIELECTRIC STRUCTURES

Recently, it was established that very specific nonlinear regimes can be achieved due to magnetic optical response of artificial "meta-atoms" [156]. This picture is at large adapted in the microwave range, and a vast number of research groups are engaged in utilizing tailored nonlinear response of metamaterials, as shown in the recent review [157]. When nonlinearities of both electric and magnetic origin are present, nonlinear response can be modified substantially being accompanied

by nonlinear interference, magnetoelectric coupling, and wave mixing effects [158, 159]. In particular, the interference between the electric and magnetic nonlinear contributions can lead to unidirectional harmonic generation from an ultra-thin metasurface [158] and "non-reciprocal" nonlinear scattering [158] from a symmetric subwavelength nanoelement [160]. The idea of magnetic nonlinearities evolves, being further elaborated by the optics community. It finds implementations in double-layer fishnet structures [155, 161–163], coupled metal nanodisks [154, 164], and nanostrips [165]. These coupled plasmonic structures sustain antisymmetric oscillations of electron plasma leading to the magnetic-type resonances and the associated enhancement of the nonlinear response. The dissimilar electric and magnetic contributions to the nonlinear response are then disclosed by spectrally resolved measurements and multipolar decomposition of the generated harmonic signal. In Ref. [154], such analysis was performed for SHG observed from a metasurface composed of metal-dielectric-metal nanodisks, see Fig. 3(a). The resonant excitation of the magnetic optical mode in composite nanoparticles was shown to govern the efficient nonlinear conversion of the multipolar origin, being a superposition of nonlinearly-induced magnetic dipole and electric quadrupole modes with a suppressed contribution from the electric dipole mode. Phenomenological macroscopic description, developed in Ref. [164], established a connection of the resonant enhancement of SHG in such "nanosandwiches" under the excitation of the MD resonance with the dominant role of the nonlinear magnetic-dipole polarization driven by the χ^{emm} susceptibility. Here, the first index in the superscript corresponds to the electric polarization induced at SH frequency, while the two other denote the magnetic fundamental fields.

Ref. [155] reports on the experimental identification of multipolar contributions in the THG signal from a metal-dielectric-metal layered fishnet metamaterial illuminated with a focused pump beam in the vicinity of the magnetic resonance, see Fig. 3(b). Previously, the electric and magnetic dipole resonances in fishnets were shown to be responsible for notably distinct THG angular patterns [162]. The metamaterial studied in Ref. [155] consists of Au/MgF₂/Au structure perforated periodically with an array of holes, and the magnetic response is attained due to antiparallel currents in the top and bottom metal layers. The detected THG radiation pattern, measured by a Fourier imaging technique, was proven to be a result of the interference of the electric dipolar, magnetic dipolar and electric quadrupolar modes [155].

ALL-DIELECTRIC NANOSTRUCTURES

Ohmic losses, heating and low damage thresholds pose substantial restrictions on the achievable performance of the nonlinear plasmonic devices exploiting metallic components, thus limiting their practical use. Nanoparticles

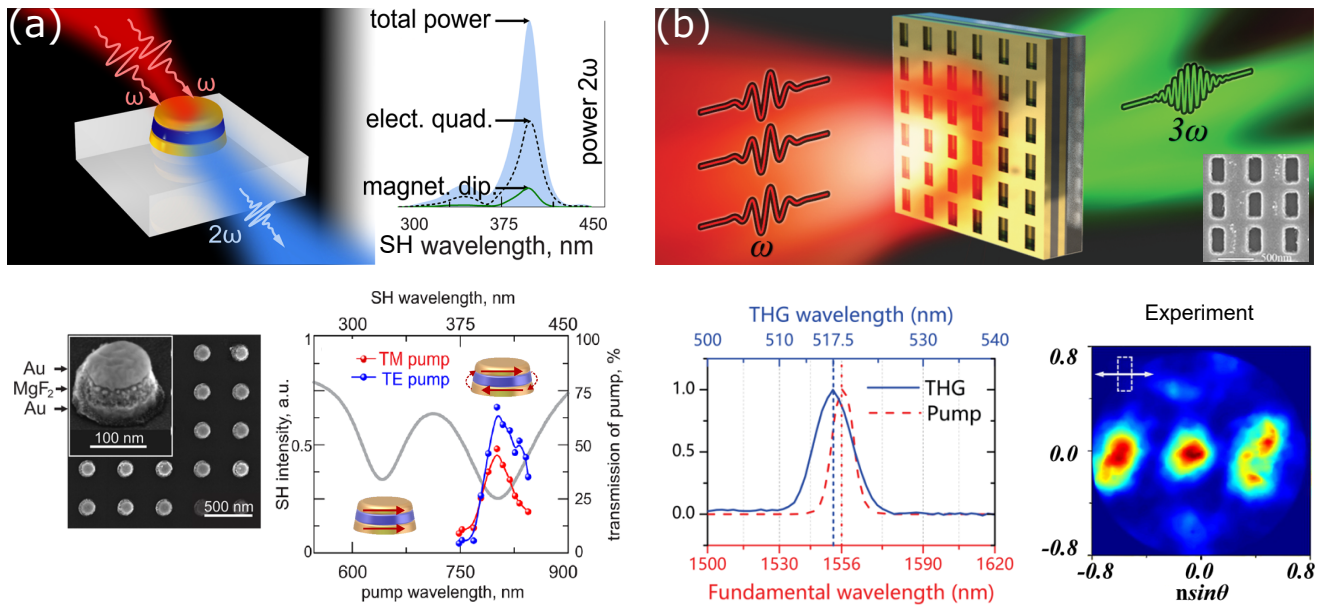


Figure 3. (a) Top left: Schematic view of the experiment on SHG with a metasurface of metal-dielectric disk-like nanoparticles made of Au/MgF₂/Au layers. Top right: Multipole decomposition of SH signal numerically calculated for the TE-polarized pump at the oblique 30° incidence. Bottom left: SEM image of a fabricated metasurface. Bottom right: Linear transmission of the metasurface (gray) at normal incidence and second-harmonic spectra for TM- and TE-polarized pump waves (red and blue) measured for the incident angle of 30°. Adopted from Ref. [154]. The insets illustrate the electric current distribution in a single composite nanoparticle in ED and MD resonant modes associated with two dips in transmission. (b) Top: Schematic of the experiment on the resonantly enhanced THG from a fishnet metamaterial, exhibiting a magnetic response. The inset shows a scanning electron micrograph image of the sample. Bottom left: Measured THG (solid blue) and pump (dashed red) spectra, normalized to maxima. Bottom right: back-focal-plane Fourier image of TH radiation. Adopted from Ref. [155].

made of high-refractive-index dielectrics and semiconductors (such as germanium, tellurium, GaAs, AlGaAs, GaP, silicon), which do not suffer from large intrinsic absorption at the visible, infrared and telecom frequencies, are emerging as a promising alternative to plasmonic nanostructures for nanophotonic applications [166, 167]. Such high-permittivity nanoparticles exhibit strong interaction with light due to the excitation of the Mie-type resonances they sustain [168–171]. Both these electric and magnetic resonances can be spectrally controlled and engineered independently, and therefore all-dielectric nanostructures offer unique opportunities for the study of nonlinear effects owing to low losses in combination with multipolar optical response of both electric and magnetic nature. Utilizing the Mie-type resonances in resonant subwavelength dielectric geometries has been recently recognized a promising strategy to gain high efficiencies of nonlinear processes at low mode volumes and design novel functionalities originating from the optically-induced magnetic response [47, 172–185]. Particularly, optically magnetic dielectric nanostructures are shown to significantly enhance nonlinear conversion, with the high enhancement observed for excitation of the magnetic dipole resonance.

Remarkably, the observation of highly localized fundamental magnetic dipolar mode characterized by circular displacement currents excited in spherical silicon parti-

cles of sub-micrometer size in the visible spectrum [186, 187] has led to the development of “magnetic light” concept, which triggers the whole research direction of *all-dielectric nanophotonics* [167, 188]. In most previous works on trapped magnetic resonances, silicon was the primary focus of the material [18, 33, 186, 187, 189–191] thanks to its CMOS compatibility, low cost and well-established fabrication methods. Along with a moderately high refractive index, silicon, both crystalline and amorphous, being a centrosymmetric material with inhibited quadratic nonlinearity, possesses however a strong bulk third-order optical susceptibility $\chi_b^{(3)}$ [192–200], nearly 200 larger than that of silica; therefore strong nonlinear phenomena can be anticipated in the optical response of silicon nanoparticles. Figures 4(a–d) present a few examples of the recent experimental study of nonlinear optical properties of silicon-based nanoparticles, their clusters, and metasurfaces.

Experimental studies of third-harmonic generation. In the pioneering work [172], it was experimentally confirmed that a strong enhancement of THG can be achieved in isolated silicon nanodisks and their arrays optically pumped in the vicinity of the magnetic dipolar resonance by using THG microscopy and THG spectroscopy techniques. The MD resonance is characterized by the significantly enhanced local fields tightly bound within the volume of nanoscale resonators. Since

the induced volume nonlinear source, third-order polarization $\mathbf{P}_{\text{bulk}}^{(3\omega)}$, scales with the local electric field $\mathbf{E}_{\text{loc}}^{(\omega)}$ cubed, $\mathbf{P}_{\text{bulk}}^{(3\omega)} = \varepsilon_0 \chi_b^{(3)} \mathbf{E}_{\text{loc}}^{(\omega)3}$, a considerable enhancement of THG is expected from the nanodisks pumped by the resonant laser radiation. In the experiment, silicon nanodisks placed on silica were subject to an intense femtosecond laser pulse train with frequency close to the magnetic dipole resonance. Analyzing the transmitted signal at TH, it was found that the resonant THG response from silicon nanodisks prevails by the factor of up to 100 over the THG from the bulk silicon slab. The generated 420 nm radiation was bright enough to be observed by a naked eye under the table-lamp illumination conditions, see Fig. 4(a).

Combining nanodisks into oligomers provides another degree of freedom in tailoring the nonlinear optical response. Particularly, strong reshaping of the third-harmonic spectra was observed from trimers of silicon nanodisks with varying interparticle spacings [174]. Complex multipeak patterns in measured THG spectra were substantiated by interference of the nonlinearly generated TH waves radiated by different parts of the sample and augmented by an interplay between the electric and the magnetic dipolar resonances in the nanodisks.

Optical nonlinearities can be further enhanced in finite nanoparticle clusters through the excitation of high-quality collective modes of the magnetic nature. Combining dielectric particles in oligomers may lead to the formation of collective modes with different lifetimes limited by radiative losses mainly, in a striking contrast to deeply subwavelength plasmonic analogues. Such multiresonant dielectric nanostructures can be designed to support high-quality modes of different symmetries, amplifying nonlinear optical effects. In this context, Ref. [182] presents the study of THG from quadrumers composed of four identical silicon nanodisks. Nontrivial wavelength and angular dependencies of the generated harmonic signal were observed, featuring a high enhancement of the nonlinear response associated with a specific type of the magnetic Fano resonance in oligomeric dielectric systems. First predicted in Ref. [201], this Fano resonance arises due to the magneto-electric dipole coupling in individual quadrumers. The measured linear transmission displayed in Fig. 4(b) shows a broad transmission dip and a sharp Fano-like line shape at longer wavelengths. They are attributed to the dominant resonant excitation of different collective modes in the quadrumers. Both resonances are characterized by pronounced magnetic dipolar excitations in the disks and significant local field enhancement and thereby they are accompanied by a substantial increase of the third-harmonic signal, as compared to that from both optically-decoupled disks and an unstructured silicon film of the same thickness.

Noticeably, such mechanism for the THG enhancement in a single unit cell of all-dielectric metasurfaces is different from that reported in Ref. [176], where the efficient THG is driven by a high-quality resonance, achieved in a

two-dimensional array of coupled silicon disks and bars, which stems from collective bright and dark modes of the lattice [see Fig. 4(c)]. In the latter design, nanobars with long axes parallel to the E-polarization of a normally incident radiation and exhibiting electric dipole resonances effectively couple energy from the incident wave into the dark out-of-plane magnetic dipole modes of neighboring silicon disks. A sharp peak in the measured transmittance spectra indicates the Fano interference featuring a resonance with an experimental Q -factor of 466. The associated strong enhancement of the local electric field trapped within the disks gives rise to THG amplification factor of 1.5×10^5 with respect to the unpatterned silicon film, leading to the conversion efficiency on the order of 10^{-6} , which is the largest value reported for THG on nanoscale using comparable pump energies [176, 184].

A simple disk geometry of dielectric nanoparticles appears especially attractable for experimental studies of resonant nonlinear effects because the positions of both their electric and magnetic Mie-type resonances can be easily tuned by varying the aspect ratio [202]. For instance, the efficient excitation of the magnetic dipole mode requires sufficient field retardation throughout the nanodisk to drive the displacement current loop. This suggests that if the particle gets shallow enough, ED and MD resonances become overlapped gradually expelling the in-plane MD mode. Ref. [184] demonstrates that THG in thin Ge nanodisks under normally incident laser excitation can be boosted via the nonradiative anapole mode (AM). This AM is accompanied by the pronounced dip in scattering occurring from destructive far-field interference of the electric and toroidal dipole moments, and its physics can be inferred from the Fano resonance mechanism [203]. The AM, which emerges for low enough aspect ratios, efficiently confines the electric energy inside the disks, which is similar to the performance of MD mode in thicker disks. The TH conversion at the anapole mode from a germanium disks array was measured to outperform that at the radiative electric dipolar modes, spectrally surrounding AM, by about one order of magnitude.

Theoretical approach. Analytical and numerical analysis of the resonant THG from high-index dielectric nanoparticles was performed in Ref. [47]. This work discusses the basic features and multipolar nature of the nonlinear scattering near the Mie-type optical resonances from simple nanoparticle geometries, such as spheres and disks, with a focus on silicon. Considering a model of a high-permittivity spherical dielectric particle excited in the vicinity of the magnetic dipole resonance, analytical expressions for the electromagnetic field generated at the tripled frequency are derived, and it is shown that the TH radiation pattern can be treated as a result of interference of a magnetic dipole and magnetic octupole, which is also confirmed by means of full-wave numerical simulations carried out in COMSOL, see Fig. 5. Besides, in compliance with experimental findings [172, 174–176], the efficiency of THG at the MD resonance is noted to

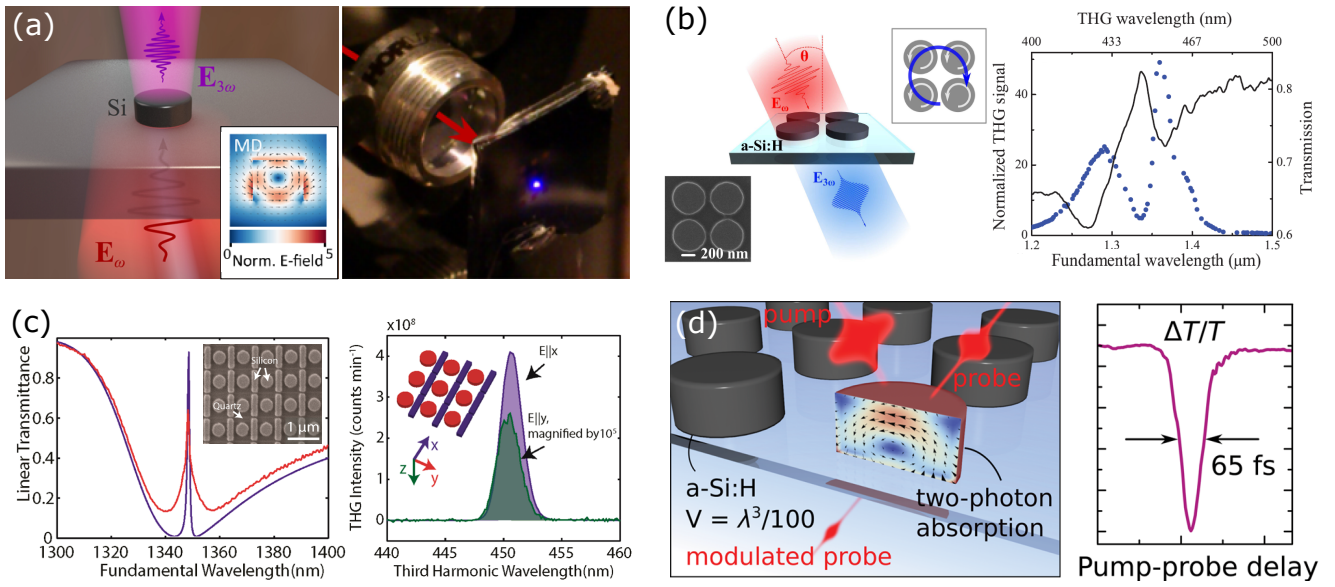


Figure 4. (a) Left: Illustration of THG from silicon nanodisks driven by the magnetic dipolar resonance excited in the disks by the impinging laser light at the fundamental frequency. Superimposed is exemplary near-field distribution of the induced electric field in a disk at MD resonance. Right: A photographic image of the eye-visible generated radiation from the nanodisks sample. Adopted from Ref. [172]. (b) Left: Schematic illustration of the resonant THG from silicon quadrumers of four a-Si:H nanodisks with SEM image of the sample in the bottom left corner. Rotating arrows picturize the origin of the magnetic Fano resonance in quadrumers: two coupled magnetic-like modes formed by out-of-plane magnetic dipoles and circulating displacement current produced by in-plane electric dipoles give rise to the Fano interference. For details, see Ref. [201]. Right: THG spectroscopy of a-Si:H quadrumers on a glass substrate. Shown are experimental transmission (black line) and THG (blue dots) spectra of the sample excited by obliquely incident s-polarized radiation at the angle of 45° . TH power is plotted normalized to the spectrum of a bare a-Si:H film. After Ref. [182]. (c) Left: Simulated (blue) and experimentally measured (red) transmission spectra of the silicon Fano-resonant metasurface with the Fano peak at the wavelength of 1350 nm. SEM image of the fabricated structure is shown in the inset. Right: Third harmonic spectra of the metasurface excited by the incident electric field polarized along the long (x -) and short (y -) axes of the bars, respectively. Adopted from Ref. [176]. (d) Ultrafast all-optical switching in resonant silicon nanodisks: (left) schematic of the experiment: a-Si disc 250 nm in diameter is capable of switching optical pulses at femtosecond rates; (right) measured modulation of the probe pulse transmittance as a function of time delay between the probe and pump pulses at low pump powers. Taken from Ref. [175].

significantly exceed that at the ED resonance. Remarkably, due to a larger mode volume of the magnetic Mie mode compared to the electric mode of the same order, the magnetic dipole resonance also superiorly enhances Raman scattering by individual silicon nanospheres [181]. In addition, the approaches for manipulating and directing the resonantly enhanced nonlinear emission by changing shapes and combining dielectric nanoparticles in oligomers are demonstrated. This concept is illustrated with an example of a nanoparticle trimer composed of a symmetric dimer of identical silicon spheres placed nearby a smaller nanoparticle. Interparticle interaction influences the multipolar content of the field scattered by a trimer, and the resultant constructive interference between the excited multipoles may provide high directivity of both the linear and nonlinear scattering simultaneously. Alternatively, the preferential backward/forward directionality of THG can be attained for a silicon nanodisk of the adjusted aspect ratio exhibiting spectrally overlapped magnetic and electric dipole resonances.

Ultrafast switching. Silicon nanoparticles employed

as nonlinear Mie-type cavities furthermore offer a platform for engineering compact and very speedy photonic switches. In Ref. [175], the authors distinguish three basic classes of nonlinear phenomena responsible for the optical self-action effect in silicon: (i) Kerr-type processes, including nonlinear refraction and two-photon absorption (TPA), (ii) free carriers (FC) generation, and (iii) thermo-optical effect. They were able to design a metasurface of amorphous silicon nanodisks, illustrated in Fig. 4(d), where the undesirable free-carrier effects, which are generally slow and pose serious restrictions on the speed of signal conversion, are suppressed, leaving the dominant fast TPA contribution in the nonlinear response. This silicon-based metasurface allowed achieving strong self-modulation of femtosecond pulses with a depth of 60% at picojoule-per-nanodisk pump energies. Pump-probe measurements demonstrated that switching in the nanodisks can be governed by pulse-limited 65 fs-long two-photon absorption being enhanced by a factor of 80 with respect to the unstructured silicon film. This result represents an important step towards novel and efficient active photonic devices, such as transis-

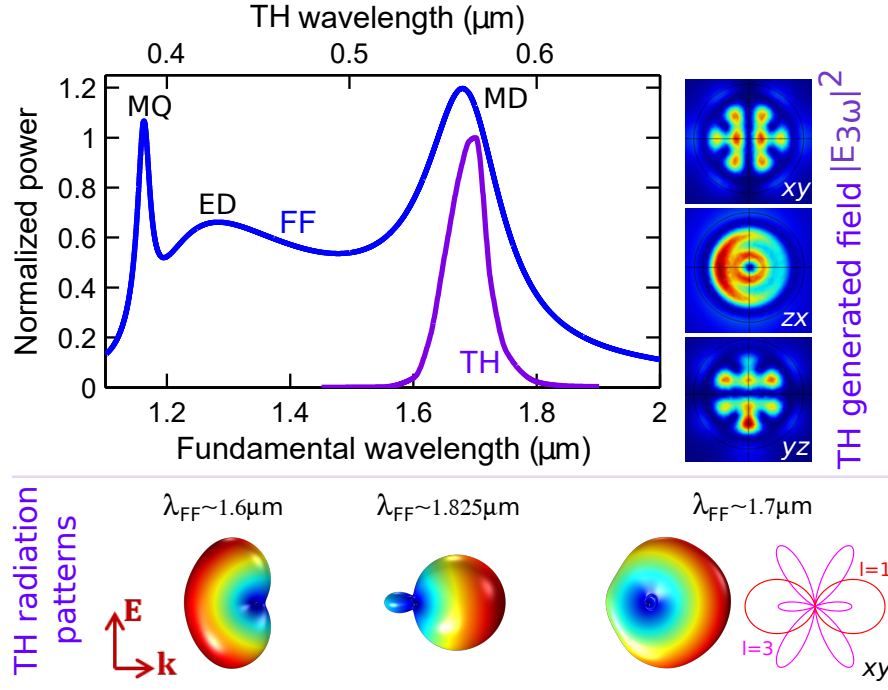


Figure 5. Spectra of the normalized scattered FF (blue) and radiated TH (purple) powers calculated numerically for a spherical dielectric particle of radius 230 nm and refractive index 3.5 excited by a linearly polarized plane wave with electric field directed along the x axis. Labeled are the positions of Mie resonances (MQ, ED and MD) in the linear scattering. Intensity maps show spatial distributions of the TH field generated near MD resonance in different cross-sections. Bottom: transformations of the TH radiation pattern with switching directionality. Within the broad MD resonance, both magnetic dipole and magnetic octupole contribute to the THG peak, that determines predominantly axially symmetric emission profile (right) and a six-petalled TH near-field structure. The xy cuts of radiation patterns for the corresponding pure magnetic dipole, $l = 1$ (red) and magnetic octupole, $l = 3$ (pink) are depicted in the polar plot. Images are adopted from Ref. [47].

tors and logic elements to be built in integrated circuits [178]. Such switching speeds potentially allow for creating data transmission and processing devices operating at tens and hundreds terabits per second. Similar to Ref. [175], Kerr and TPA effect-based transmission modulation was reported for a Fano-resonant metasurface in Ref. [176]. Nonlinear light manipulation by scattering diagram and spectra of individual silicon nanoparticles also envisions interesting possibilities for all-optical routing. In Ref. [179], it was demonstrated, both theoretically and experimentally, that ultrafast transient modulation of the dielectric permittivity due to variation of free-carrier (electron-hole plasma) density in silicon, induced via its photoexcitation by fs laser irradiation, significantly alters scattering behavior of a silicon nanoparticle, supporting a magnetic dipole resonance. Later, accelerated reconfiguration of a radiation pattern from dipole-like to unidirectional (Huygens-source scattering) regime mediated by ultrafast (with times scales of about 2.5 ps) generation of electron-hole plasma during laser pulse-nanoantenna interaction was described in Ref. [183].

Second-harmonic generation. For efficient second-order nonlinear applications, advantageous can be excitation of low-order Mie modes in nanoantennas made of high-permittivity noncentrosymmetric semiconductors.

While in plasmonic nanoparticles the second-order nonlinear response is dominated by surface nonlinearities enhanced by plasmon resonances, in high-index dielectric nanostructures the bulk nonlinearity may dominate the optical nonlinear interaction in volume, giving rise to better conversion efficiency. In Ref. [177] the disk-shaped nanoantenna made of aluminum gallium arsenide (AlGaAs) is designed for SHG at near-IR wavelengths. The authors consider this choice of material favorable because AlGaAs possesses a large volume quadratic susceptibility and parasitic TPA effects can be avoided at wavelengths close to 1.55 μm by engineering the Al molar fraction in the alloy composition. The second-order bulk nonlinear susceptibility tensor of AlGaAs, possessing a zinc blende crystalline structure, is anisotropic and contains only off-diagonal elements $\chi_{ijk}^{(2)}$ with $i \neq j \neq k$. Thus, in the principal-axis system of the crystal, the i th component of the nonlinear source polarization at SH frequency is given by $P_i^{(2\omega)} = \varepsilon_0 \chi_{ijk}^{(2)} E_j^{(\omega)} E_k^{(\omega)}$. Figure 6 shows that the maximum SHG efficiency is achieved for a pump wavelength of 1675 nm, which is close to the magnetic dipole resonance wavelength, and predicted to reach values as high as 10^{-3} at 1 GW/cm². The conversion efficiency strongly depends on the overlap between the induced nonlinear source and modes generated at SH

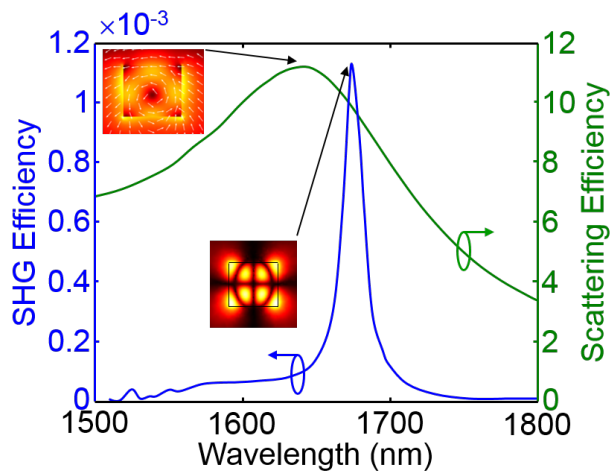


Figure 6. SHG (blue line) and linear scattering (green line) efficiencies as functions of the pump wavelength calculated for a cylindrical AlGaAs nanoantenna with a radius of 225 nm and a height 400 nm in air. Insets show profiles of the electric field amplitude in a E-plane cross-section cut through the center of the cylinder, which correspond to the maxima of two dependencies dominated by MD and EQ modes, respectively. Adopted from Refs. [177, 180].

frequency, and its peak appears slightly shifted from the resonance seen in the linear scattering. The SH nonlinear current distribution resembles an electric quadrupole in this case, and pronounced quadrupolar lobes can be recognized in the multilobe SH far-field radiation pattern [177, 180]. In the recent experiment, SH conversion efficiency exceeding 10^{-5} has been measured for AlGaAs nanocylinders with an optimized geometry pumped at the wavelength of $1.55 \mu\text{m}$ [185]. Ref. [180] further theoretically discusses shaping SH radiation profile of AlGaAs cylindrical nanoantennas through the engineered multipolar interference by manipulating the pump beam (polarization state, incidence angle, spatial structure) and by changing the disk geometry. In particular, whereas no SH emission can be generated by the AlGaAs nanodisk in the normal forward or backward direction under normal excitation because of the structural symmetry and properties of the AlGaAs nonlinear susceptibility, using a pump beam at tilted incidence is beneficial for obtaining SH signal in the normal directions and increasing the detectable SH power that can be measured through a finite numerical aperture microscope objective.

CONCLUDING REMARKS AND OUTLOOK

We have discussed multipolar nonlinear effects in resonant metallic, metal-dielectric, and all-dielectric photonic structures. The studies of nonlinear phenomena accompanying the propagation and scattering of light in nanostructured media have been stimulated by a rapid progress in nanofabrication techniques, such as electron beam lithography and wet chemical growth, and a growing interest in photonic metamaterials with optically-induced magnetic response. The approach based on the multipolar expansion of the electromagnetic fields is closely associated with the Mie scattering theory, and it provides an unified description and useful insights into the physics underlying the nonlinear processes with resonantly driven nanoparticles and nanoparticle clusters. The realization of submicron structures of simple geometries exhibiting intense nonlinear response is eminently promising for the optics-based data manipulation and storage technology, sensing applications, and topological photonics.

While the extensive theoretical and experimental studies of nonlinear optical properties of metallic nanoparticles laid the foundation of contemporary nonlinear nanoplasmonics, in many cases appealing to the electric dipole resonances, all-dielectric systems have recently been demonstrated to offer stronger nonlinear effects and novel functionalities enabled by pronounced magnetic dipole and higher-order Mie-type resonances. The coexistence of strong electric and magnetic resonances and their interference in high-index dielectric and semiconductor nanostructures bring new physics to simple geometries, opening unique prospects for constructing optical nanoantennas and metasurfaces with reduced dissipative losses and considerable enhancement of the nonlinearly generated fields. These recent developments suggest intriguing opportunities for a design of nonlinear subwavelength light sources with reconfigurable radiation characteristics and engineering large effective optical nonlinearities at the nanoscale, which could have important implications for novel nonlinear photonic metadevices operating beyond the diffraction limit.

Acknowledgements. The authors thank M. Kauranen, A. Zayats, H. Giessen, O. J. F. Martin, N. Panou, V. Valev and C. De Angelis for useful discussions and suggestions. This work was supported by the Australian Research Council and RFBR Grant No. 16-02-00547.

-
- [1] L. Novotny and B. Hecht, *Principles of Nano-Optics* (Cambridge University Press, New York, 2007).
 - [2] V. M. Shalaev and S. Kawata, eds., *Nanophotonics with Surface Plasmons* (Elsevier Science, 2007).
 - [3] M. L. Brongersma and P. G. Kik, eds., *Surface Plasmon Nanophotonics* (Springer Netherlands, 2007).

- [4] D. K. Gramotnev and S. I. Bozhevolnyi, "Plasmonics beyond the diffraction limit," *Nat. Photon.* **4**, 83–91 (2010).
- [5] V. M. Menon, L. I. Deych, and A. A. Lisyansky, "Nonlinear optics: Towards polaritonic logic circuits," *Nat. Photon.* **4**, 345–346 (2010).

- [6] D. A. B. Miller, “Are optical transistors the logical next step?” *Nat. Photon.* **4**, 3–5 (2010).
- [7] S. A. Maier, ed., *Plasmonics: Fundamentals and Applications* (Springer-Verlag, 2007).
- [8] L. Cao and M. L. Brongersma, “Active plasmonics: Ultrafast developments,” *Nat. Photon.* **3**, 12–13 (2009).
- [9] S. Kawata, Y. Inouye, and P. Verma, “Plasmonics for near-field nano-imaging and superlensing,” *Nat. Photon.* **3**, 388–394 (2009).
- [10] N. Liu, M. L. Tang, M. Hentschel, H. Giessen, and A. P. Alivisatos, “Nanoantenna-enhanced gas sensing in a single tailored nanofocus,” *Nat. Mater.* **10**, 631–636 (2011).
- [11] A. A. Maradudin, J. R. Sambles, and W. L. Barnes, *Modern Plasmonics* (Elsevier B.V., Poland, 2014).
- [12] D. Rodrigo, O. Limaj, D. Janner, D. Etezadi, F. J. G. de Abajo, V. Pruneri, and H. Altug, “Mid-infrared plasmonic biosensing with graphene,” *Science* **349**, 165–168 (2015).
- [13] J. A. Schuller, E. S. Barnard, W. Cai, Y. C. Jun, J. S. White, and M. L. Brongersma, “Plasmonics for extreme light concentration and manipulation,” *Nat. Mater.* **9**, 193–204 (2010).
- [14] V. Klimov, *Nanoplasmonics: Fundamentals and Applications* (Pan Stanford Publishing, Singapore, 2012).
- [15] R. W. Boyd, *Nonlinear Optics, 3rd ed.* (Elsevier, New York, 2008).
- [16] L. Novotny and N. van Hulst, “Antennas for light,” *Nat. Photonics* **5**, 83–90 (2011).
- [17] A. E. Krasnok, I. S. Maksymov, A. I. Denisyuk, P. A. Belov, A. E. Miroshnichenko, C. R. Simovski, and Y. S. Kivshar, “Optical nanoantennas,” *Phys.-Usp.* **56**, 539–564 (2013).
- [18] I. Staude, A. E. Miroshnichenko, M. Decker, N. T. Fofang, S. Liu, E. Gonzales, J. Dominguez, T. S. Luk, D. N. Neshev, I. Brener, and Y. Kivshar, “Tailoring directional scattering through magnetic and electric resonances in subwavelength silicon nanodisks,” *ACS Nano* **7**, 7824–7832 (2013).
- [19] A. E. Krasnok, P. A. Belov, A. E. Miroshnichenko, A. I. Kuznetsov, B. S. Lukyanchuk, and Y. S. Kivshar, “All-dielectric optical nanoantennas,” in “Progress in Compact Antennas,” (InTech, 2014).
- [20] A. K. Sarychev and V. M. Shalaev, *Electrodynamics of Metamaterials* (World Scientific, Singapore, 2007).
- [21] A. Boltasseva and V. M. Shalaev, “Fabrication of optical negative-index metamaterials: Recent advances and outlook,” *Metamaterials* **2**, 1–17 (2008).
- [22] W. Cai and V. Shalaev, *Optical Metamaterials* (Springer Science + Business Media, 2010).
- [23] J. D. Jackson, *Classical electrodynamics* (Wiley, New York, 1999).
- [24] C. F. Bohren and D. R. Huffman, *Absorption and Scattering of Light by Small Particles* (Wiley, New York, 1983).
- [25] J. I. Dadap, J. Shan, and T. F. Heinz, “Theory of optical second-harmonic generation from a sphere of centrosymmetric material: small-particle limit,” *J. Opt. Soc. Am. B* **21**, 1328 (2004).
- [26] J. Petschulat, A. Chipouline, A. Tünnermann, T. Pertsch, C. Menzel, C. Rockstuhl, and F. Lederer, “Multipole nonlinearity of metamaterials,” *Phys. Rev. A* **80**, 063828 (2009).
- [27] N. Liu, H. Liu, S. Zhu, and H. Giessen, “Stereometamaterials,” *Nature Photon.* **3**, 157–162 (2009).
- [28] S. Mühlig, C. Menzel, C. Rockstuhl, and F. Lederer, “Multipole analysis of meta-atoms,” *Metamaterials* **5**, 64–73 (2011).
- [29] G. Gonella and H.-L. Dai, “Determination of adsorption geometry on spherical particles from nonlinear Mie theory analysis of surface second harmonic generation,” *Phys. Rev. B* **84**, 121402 (2011).
- [30] P. Grahn, A. Shevchenko, and M. Kaivola, “Electromagnetic multipole theory for optical nanomaterials,” *New J. Phys.* **14**, 093033 (2012).
- [31] W. Liu, A. E. Miroshnichenko, D. N. Neshev, and Y. S. Kivshar, “Broadband unidirectional scattering by magneto-electric core-shell nanoparticles,” *ACS Nano* **6**, 5489–5497 (2012).
- [32] S. G. Rodrigo, H. Harutyunyan, and L. Novotny, “Coherent control of light scattering from nanostructured materials by second-harmonic generation,” *Phys. Rev. Lett.* **110**, 177405 (2013).
- [33] Y. H. Fu, A. I. Kuznetsov, A. E. Miroshnichenko, Y. F. Yu, and B. Luk’yanchuk, “Directional visible light scattering by silicon nanoparticles,” *Nat. Commun.* **4**, 1527 (2013).
- [34] E. Poutrina, A. Rose, D. Brown, A. Urbas, and D. R. Smith, “Forward and backward unidirectional scattering from plasmonic coupled wires,” *Opt. Express* **21**, 31138 (2013).
- [35] A. E. Krasnok, C. R. Simovski, P. A. Belov, and Y. S. Kivshar, “Superdirective dielectric nanoantennas,” *Nanoscale* **6**, 7354 (2014).
- [36] D. A. Smirnova, I. V. Shadrivov, A. E. Miroshnichenko, A. I. Smirnov, and Y. S. Kivshar, “Second-harmonic generation by a graphene nanoparticle,” *Phys. Rev. B* **90**, 035412 (2014).
- [37] R. B. Davidson II, J. I. Ziegler, G. Vargas, S. M. Avanesyan, Y. Gong, W. Hess, and R. F. Haglund Jr., “Efficient forward second-harmonic generation from planar archimedean nanospirals,” *Nanophotonics* **4**, 2 (2015).
- [38] D. Dregely, K. Lindfors, M. Lippitz, N. Engheta, M. Totzeck, and H. Giessen, “Imaging and steering an optical wireless nanoantenna link,” *Nat. Commun.* **5**, 5354 (2014).
- [39] I. Liberal, I. Ederra, R. Gonzalo, and R. W. Ziolkowski, “Superbackscattering from single dielectric particles,” *J. Opt.* **17**, 072001 (2015).
- [40] M. Kerker, D.-S. Wang, and C. L. Giles, “Electromagnetic scattering by magnetic spheres,” *J. Opt. Soc. Am. B* **73**, 765 (1983).
- [41] W. Liu, J. Zhang, B. Lei, H. Ma, W. Xie, and H. Hu, “Ultra-directional forward scattering by individual core-shell nanoparticles,” *Opt. Express* **22**, 16178 (2014).
- [42] I. M. Hancu, A. G. Curto, M. Castro-López, M. Kuttge, and N. F. van Hulst, “Multipolar interference for directed light emission,” *Nano Lett.* **14**, 166–171 (2014).
- [43] R. R. Naraghi, S. Sukhov, and A. Dogariu, “Directional control of scattering by all-dielectric core-shell spheres,” *Opt. Lett.* **40**, 585 (2015).
- [44] R. Alaee, R. Filter, D. Lehr, F. Lederer, and C. Rockstuhl, “A generalized Kerker condition for highly directive nanoantennas,” *Opt. Lett.* **40**, 2645 (2015).
- [45] S. Roke, M. Bonn, and A. V. Petukhov, “Nonlinear optical scattering: The concept of effective susceptibility,” *Phys. Rev. B* **70**, 115106 (2004).
- [46] K. O’Brien, H. Suchowski, J. Rho, A. Salandrino,

- B. Kante, X. Yin, and X. Zhang, “Predicting nonlinear properties of metamaterials from the linear response,” *Nat. Mater.* **14**, 379–383 (2015).
- [47] D. A. Smirnova, A. B. Khanikaev, L. A. Smirnov, and Y. S. Kivshar, “Multipolar third-harmonic generation driven by optically induced magnetic resonances,” *ACS Photonics* (2016).
- [48] K. Thyagarajan, S. Rivier, A. Lovera, and O. J. Martin, “Enhanced second-harmonic generation from double resonant plasmonic antennae,” *Opt. Express* **20**, 12860 (2012).
- [49] M. Navarro-Cia and S. A. Maier, “Broad-band near-infrared plasmonic nanoantennas for higher harmonic generation,” *ACS Nano* **6**, 3537–3544 (2012).
- [50] H. Aouani, M. Navarro-Cia, M. Rahmani, T. P. H. Sidiropoulos, M. Hong, R. F. Oulton, and S. A. Maier, “Multiresonant broadband optical antennas as efficient tunable nanosources of second harmonic light,” *Nano Lett.* **12**, 4997–5002 (2012).
- [51] P. Ginzburg, A. Krasavin, Y. Sonnefraud, A. Murphy, R. J. Pollard, S. A. Maier, and A. V. Zayats, “Nonlinearly coupled localized plasmon resonances: Resonant second-harmonic generation,” *Phys. Rev. B* **86**, 085422 (2012).
- [52] M. Celebrano, X. Wu, M. Baselli, S. Großmann, P. Biagioni, A. Locatelli, C. D. Angelis, G. Cerullo, R. Oselame, B. Hecht, L. Duò, F. Ciccacci, and M. Finazzi, “Mode matching in multiresonant plasmonic nanoantennas for enhanced second harmonic generation,” *Nature Nanotech* **10**, 412–417 (2015).
- [53] F. Bassani and V. Lucarini, “General properties of optical harmonic generation from a simple oscillator model,” *Nouv Cim D* **20**, 1117–1125 (1998).
- [54] E. Poutrina, D. Huang, Y. Urzhumov, and D. R. Smith, “Nonlinear oscillator metamaterial model: Numerical and experimental verification,” *Opt. Express* **19**, 8312 (2011).
- [55] R. C. Miller, “Optical second-harmonic generation in piezoelectric crystals,” *Appl. Phys. Lett.* **5**, 17 (1964).
- [56] C. Garrett and F. Robinson, “Miller’s phenomenological rule for computing nonlinear susceptibilities,” *IEEE J. Quantum Electron* **2**, 328–329 (1966).
- [57] J. Butet and O. J. F. Martin, “Evaluation of the nonlinear response of plasmonic metasurfaces: Miller’s rule, nonlinear effective susceptibility method, and full-wave computation,” *J. Opt. Soc. Am. B* **33**, A8 (2016).
- [58] M. Hentschel, T. Utikal, H. Giessen, and M. Lippitz, “Quantitative modeling of the third-harmonic emission spectrum of plasmonic nanoantennas,” *Nano Lett.* **12**, 3778–3782 (2012).
- [59] B. Metzger, M. Hentschel, M. Lippitz, and H. Giessen, “Third-harmonic spectroscopy and modeling of the nonlinear response of plasmonic nanoantennas,” *Opt. Lett.* **37**, 4741 (2012).
- [60] B. Metzger, T. Schumacher, M. Hentschel, M. Lippitz, and H. Giessen, “Third harmonic mechanism in complex plasmonic Fano structures,” *ACS Photonics* **1**, 471–476 (2014).
- [61] R. Czaplicki, J. Mäkitalo, R. Siikanen, H. Husu, J. Lehtolahti, M. Kuittinen, and M. Kauranen, “Second-harmonic generation from metal nanoparticles: Resonance enhancement versus particle geometry,” *Nano Lett.* **15**, 530–534 (2015).
- [62] G. Bautista and M. Kauranen, “Vector-field nonlinear microscopy of nanostructures,” *ACS Photonics* (2016).
- [63] D. de Ceglia, M. A. Vincenti, C. D. Angelis, A. Locatelli, J. W. Haus, and M. Scalora, “Role of antenna modes and field enhancement in second harmonic generation from dipole nanoantennas,” *Opt. Express* **23**, 1715 (2015).
- [64] G. D. Bernasconi, J. Butet, and O. J. F. Martin, “Mode analysis of second-harmonic generation in plasmonic nanostructures,” *J. Opt. Soc. Am. B* **33**, 768 (2016).
- [65] M. Lippitz, M. A. van Dijk, and M. Orrit, “Third-harmonic generation from single gold nanoparticles,” *Nano Lett.* **5**, 799–802 (2005).
- [66] M. Kasperczyk, S. Person, D. Ananias, L. D. Carlos, and L. Novotny, “Excitation of magnetic dipole transitions at optical frequencies,” *Phys. Rev. Lett.* **114**, 163903 (2015).
- [67] L. Cao, N. C. Panoiu, and R. M. Osgood, “Surface phase second-harmonic generation from surface plasmon waves scattered by metallic nanostructures,” *Phys. Rev. B* **75**, 205401 (2007).
- [68] S. Roke and G. Gonella, “Nonlinear light scattering and spectroscopy of particles and droplets in liquids,” *Annu. Rev. Phys. Chem.* **63**, 353–378 (2012).
- [69] M. Kauranen and A. V. Zayats, “Nonlinear plasmonics,” *Nat. Photonics* **6**, 737–748 (2012).
- [70] J. Butet, P.-F. Brevet, and O. J. F. Martin, “Optical second harmonic generation in plasmonic nanostructures: From fundamental principles to advanced applications,” *ACS Nano* **9**, 10545–10562 (2015).
- [71] P. Segovia, G. Marino, A. V. Krasavin, N. Olivier, G. A. Wurtz, P. A. Belov, P. Ginzburg, and A. V. Zayats, “Hyperbolic metamaterial antenna for second-harmonic generation tomography,” *Opt. Express* **23**, 30730 (2015).
- [72] Y. Zhang, F. Wen, Y.-R. Zhen, P. Nordlander, and N. J. Halas, “Coherent Fano resonances in a plasmonic nanocluster enhance optical four-wave mixing,” *Proc. Natl. Acad. Sci. USA* **110**, 9215–9219 (2013).
- [73] P. Biagioni, D. Brida, J.-S. Huang, J. Kern, L. Duò, B. Hecht, M. Finazzi, and G. Cerullo, “Dynamics of four-photon photoluminescence in gold nanoantennas,” *Nano Lett.* **12**, 2941–2947 (2012).
- [74] A. R. Davoyan, I. V. Shadrivov, and Y. S. Kivshar, “Self-focusing and spatial plasmon-polariton solitons,” *Opt. Express* **17**, 21732 (2009).
- [75] R. E. Noskov, P. A. Belov, and Y. S. Kivshar, “Subwavelength modulational instability and plasmon oscillons in nanoparticle arrays,” *Phys. Rev. Lett.* **108**, 093901 (2012).
- [76] R. E. Noskov, A. E. Krasnok, and Y. S. Kivshar, “Nonlinear metal-dielectric nanoantennas for light switching and routing,” *New J. Phys.* **14**, 093005 (2012).
- [77] A. D. Neira, N. Olivier, M. E. Nasir, W. Dickson, G. A. Wurtz, and A. V. Zayats, “Eliminating material constraints for nonlinearity with plasmonic metamaterials,” *Nat. Commun.* **6**, 7757 (2015).
- [78] Y. Huang, A. E. Miroshnichenko, and L. Gao, “Low-threshold optical bistability of graphene-wrapped dielectric composite,” *Sci. Rep.* **6**, 23354 (2016).
- [79] W. Fan, S. Zhang, N.-C. Panoiu, A. Abdenour, S. Krishna, R. M. Osgood, K. J. Malloy, and S. R. J. Brueck, “Second-harmonic generation from a nanopatterned isotropic nonlinear material,” *Nano Lett.* **6**, 1027–1030 (2006).

- [80] J. Lee, M. Tymchenko, C. Argyropoulos, P.-Y. Chen, F. Lu, F. Demmerle, G. Boehm, M.-C. Amann, A. Alù, and M. A. Belkin, “Giant nonlinear response from plasmonic metasurfaces coupled to intersubband transitions,” *Nature* **511**, 65–69 (2014).
- [81] Y. Zhu, X. Hu, Y. Fu, H. Yang, and Q. Gong, “Ultralow-power and ultrafast all-optical tunable plasmon-induced transparency in metamaterials at optical communication range,” *Sci. Rep.* **3**, 2338 (2013).
- [82] B. Metzger, M. Hentschel, T. Schumacher, M. Lipitz, X. Ye, C. B. Murray, B. Knabe, K. Buse, and H. Giessen, “Doubling the efficiency of third harmonic generation by positioning ITO nanocrystals into the hot-spot of plasmonic gap-antennas,” *Nano Lett.* **14**, 2867–2872 (2014).
- [83] P.-Y. Chen, C. Argyropoulos, G. D’Aguanno, and A. Alù, “Enhanced second-harmonic generation by metasurface nanomixer and nanocavity,” *ACS Photonics* **2**, 1000–1006 (2015).
- [84] D. A. Smirnova, A. E. Miroshnichenko, Y. S. Kivshar, and A. B. Khanikaev, “Tunable nonlinear graphene metasurfaces,” *Phys. Rev. B* **92**, 161406 (2015).
- [85] A. E. Minovich, A. E. Miroshnichenko, A. Y. Bykov, T. V. Murzina, D. N. Neshev, and Y. S. Kivshar, “Functional and nonlinear optical metasurfaces,” *Laser Photon. Rev.* **9**, 195–213 (2015).
- [86] T. Heinz, “Second-order nonlinear optical effects at surfaces and interfaces,” in “Nonlinear Surface Electromagnetic Phenomena,” H. Ponath and G. Stegeman, eds. (Elsevier, Amsterdam, 1991), pp. 353–416.
- [87] F. X. Wang, F. J. Rodríguez, W. M. Albers, R. Ahorinta, J. E. Sipe, and M. Kauranen, “Surface and bulk contributions to the second-order nonlinear optical response of a gold film,” *Phys. Rev. B* **80**, 233402 (2009).
- [88] G. Bachelier, J. Butet, I. Russier-Antoine, C. Jonin, E. Benichou, and P.-F. Brevet, “Origin of optical second-harmonic generation in spherical gold nanoparticles: Local surface and nonlocal bulk contributions,” *Phys. Rev. B* **82**, 235403 (2010).
- [89] D. Krause, C. W. Teplin, and C. T. Rogers, “Optical surface second harmonic measurements of isotropic thin-film metals: Gold, silver, copper, aluminum, and tantalum,” *J. Appl. Phys.* **96**, 3626 (2004).
- [90] J. E. Sipe and G. I. Stegeman, *Surface Polaritons: Electromagnetic waves at surfaces and interfaces* (North-Holland, Amsterdam, 1982).
- [91] A. Liebsch, “Second-harmonic generation at simple metal surfaces,” *Phys. Rev. Lett.* **61**, 1897–1897 (1988).
- [92] C. Ciraci, E. Poutina, M. Scalora, and D. R. Smith, “Second-harmonic generation in metallic nanoparticles: Clarification of the role of the surface,” *Phys. Rev. B* **86**, 115451 (2012).
- [93] R. Sundararaman, P. Narang, A. S. Jermyn, W. A. G. III, and H. A. Atwater, “Theoretical predictions for hot-carrier generation from surface plasmon decay,” *Nat. Commun.* **5**, 5788 (2014).
- [94] P. Ginzburg, A. V. Krasavin, G. A. Wurtz, and A. V. Zayats, “Nonperturbative hydrodynamic model for multiple harmonics generation in metallic nanostructures,” *ACS Photonics* **2**, 8–13 (2015).
- [95] A. V. Krasavin, P. Ginzburg, G. A. Wurtz, and A. V. Zayats, “Nonlocality-driven supercontinuum white light generation in plasmonic nanostructures,” *Nat. Commun.* **7**, 11497 (2016).
- [96] G. Gonella, W. Gan, B. Xu, and H.-L. Dai, “The effect of composition, morphology, and susceptibility on nonlinear light scattering from metallic and dielectric nanoparticles,” *J. Phys. Chem. Lett.* **3**, 2877–2881 (2012).
- [97] Y. Zhang, N. K. Grady, C. Ayala-Orozco, and N. J. Halas, “Three-dimensional nanostructures as highly efficient generators of second harmonic light,” *Nano Lett.* **11**, 5519–5523 (2011).
- [98] J. Dewitz, W. Hübner, and K. Bennemann, “Theory for nonlinear Mie-scattering from spherical metal clusters,” *Z. Phys. D* **37**, 75–84 (1996).
- [99] Y. Pavlyukh and W. Hübner, “Nonlinear Mie scattering from spherical particles,” *Phys. Rev. B* **70**, 245434 (2004).
- [100] A. G. F. de Beer and S. Roke, “Nonlinear Mie theory for second-harmonic and sum-frequency scattering,” *Phys. Rev. B* **79**, 155420 (2009).
- [101] S. Wunderlich, B. Schürer, C. Sauerbeck, W. Peukert, and U. Peschel, “Molecular Mie model for second harmonic generation and sum frequency generation,” *Phys. Rev. B* **84**, 235403 (2011).
- [102] J. Butet, I. Russier-Antoine, C. Jonin, N. Lascoux, E. Benichou, and P.-F. Brevet, “Nonlinear Mie theory for the second harmonic generation in metallic nanoshells,” *J. Opt. Soc. Am. B* **29**, 2213 (2012).
- [103] A. Capretti, C. Forestiere, L. D. Negro, and G. Miano, “Full-wave analytical solution of second-harmonic generation in metal nanospheres,” *Plasmonics* **9**, 151–166 (2013).
- [104] J. I. Dadap, J. Shan, K. B. Eisenthal, and T. F. Heinz, “Second-harmonic Rayleigh scattering from a sphere of centrosymmetric material,” *Phys. Rev. Lett.* **83**, 4045–4048 (1999).
- [105] C. G. Biris and N. C. Panoiu, “Second harmonic generation in metamaterials based on homogeneous centrosymmetric nanowires,” *Phys. Rev. B* **81**, 195102 (2010).
- [106] C. G. Biris and N. C. Panoiu, “Nonlinear pulsed excitation of high-Q optical modes of plasmonic nanocavities,” *Opt. Express* **18**, 17165 (2010).
- [107] B. Gallinet, J. Butet, and O. J. F. Martin, “Numerical methods for nanophotonics: standard problems and future challenges,” *Laser & Photonics Reviews* **9**, 577–603 (2015).
- [108] G. Bachelier, I. Russier-Antoine, E. Benichou, C. Jonin, and P.-F. Brevet, “Multipolar second-harmonic generation in noble metal nanoparticles,” *J. Opt. Soc. Am. B* **25**, 955 (2008).
- [109] J. Butet, G. Bachelier, I. Russier-Antoine, C. Jonin, E. Benichou, and P.-F. Brevet, “Interference between selected dipoles and octupoles in the optical second-harmonic generation from spherical gold nanoparticles,” *Phys. Rev. Lett.* **105**, 077401 (2010).
- [110] J. Butet, J. Duboisset, G. Bachelier, I. Russier-Antoine, E. Benichou, C. Jonin, and P.-F. Brevet, “Optical second-harmonic generation of single metallic nanoparticles embedded in a homogeneous medium,” *Nano Lett.* **10**, 1717–1721 (2010).
- [111] C. Forestiere, A. Capretti, and G. Miano, “Surface integral method for second harmonic generation in metal nanoparticles including both local-surface and nonlocal-bulk sources,” *J. Opt. Soc. Am. B* **30**, 2355 (2013).
- [112] J. Butet, B. Gallinet, K. Thyagarajan, and O. J. F. Mar-

- tin, “Second-harmonic generation from periodic arrays of arbitrary shape plasmonic nanostructures: a surface integral approach,” *J. Opt. Soc. Am. B* **30**, 2970 (2013).
- [113] J. Butet, S. Dutta-Gupta, and O. J. F. Martin, “Surface second-harmonic generation from coupled spherical plasmonic nanoparticles: Eigenmode analysis and symmetry properties,” *Phys. Rev. B* **89**, 245449 (2014).
- [114] T. Laroche, F. I. Baida, and D. V. Labeke, “Three-dimensional finite-difference time-domain study of enhanced second-harmonic generation at the end of an apertureless scanning near-field optical microscope metal tip,” *J. Opt. Soc. Am. B* **22**, 1045 (2005).
- [115] J. Shan, J. I. Dadap, I. Stiofkin, G. A. Reider, and T. F. Heinz, “Experimental study of optical second-harmonic scattering from spherical nanoparticles,” *Phys. Rev. A* **73**, 023819 (2006).
- [116] S.-H. Jen, G. Gonella, and H.-L. Dai, “The effect of particle size in second-harmonic generation from the surface of spherical colloidal particles. I: Experimental observations,” *J. Phys. Chem. A* **113**, 4758–4762 (2009).
- [117] J. Nappa, G. Revillod, I. Russier-Antoine, E. Benichou, C. Jonin, and P. F. Brevet, “Electric dipole origin of the second-harmonic generation of small metallic particles,” *Phys. Rev. B* **71**, 165407 (2005).
- [118] I. Russier-Antoine, E. Benichou, G. Bachelier, C. Jonin, and P. F. Brevet, “Multipolar contributions of the second harmonic generation from silver and gold nanoparticles,” *J. Phys. Chem. C* **111**, 9044–9048 (2007).
- [119] W. L. Mochán, J. A. Maytorena, B. S. Mendoza, and V. L. Brudny, “Second-harmonic generation in arrays of spherical particles,” *Phys. Rev. B* **68**, 085318 (2003).
- [120] B. Huo, X. Wang, S. Chang, M. Zeng, and G. Zhao, “Second-harmonic generation of individual centrosymmetric sphere excited by a tightly focused beam,” *J. Opt. Soc. Am. B* **28**, 2702 (2011).
- [121] F. Zeuner, M. Muldarisnur, A. Hildebrandt, J. Förstner, and T. Zentgraf, “Coupling mediated coherent control of localized surface plasmon polaritons,” *Nano Lett.* **15**, 4189–4193 (2015).
- [122] A. N. Grigorenko, M. Polini, and K. S. Novoselov, “Graphene plasmonics,” *Nat. Photon.* **6**, 749–758 (2012).
- [123] F. J. G. de Abajo, “Graphene plasmonics: Challenges and opportunities,” *ACS Photonics* **1**, 135–152 (2014).
- [124] M. Jablan, M. Soljacic, and H. Buljan, “Plasmons in graphene: Fundamental properties and potential applications,” *Proc. IEEE* **101**, 1689–1704 (2013).
- [125] M. Glazov and S. Ganichev, “High frequency electric field induced nonlinear effects in graphene,” *Phys. Rep.* **535**, 101–138 (2014).
- [126] J. D. Cox and F. J. G. de Abajo, “Electrically tunable nonlinear plasmonics in graphene nanoislands,” *Nat. Commun.* **5**, 5725 (2014).
- [127] M. T. Manzoni, I. Silveiro, F. J. G. de Abajo, and D. E. Chang, “Second-order quantum nonlinear optical processes in single graphene nanostructures and arrays,” *New J. Phys.* **17**, 083031 (2015).
- [128] J. W. Ko, S.-W. Kim, J. Hong, J. Ryu, K. Kang, and C. B. Park, “Synthesis of graphene-wrapped CuO hybrid materials by CO₂ mineralization,” *Green Chem.* **14**, 2391 (2012).
- [129] J. S. Lee, K. H. You, and C. B. Park, “Highly photoactive, low bandgap TiO₂ nanoparticles wrapped by graphene,” *Adv. Mater.* **24**, 1084–1088 (2012).
- [130] S. Sheng, L. Zhang, and G. Chen, “Low-cost fabrication of graphene ball electrodes for the amperometric detection of capillary electrophoresis,” *Electrochem. Commun.* **24**, 13–16 (2012).
- [131] B. K. Canfield, S. Kujala, K. Jefimovs, Y. Svirko, J. Turunen, and M. Kauranen, “A macroscopic formalism to describe the second-order nonlinear optical response of nanostructures,” *J. Opt. A: Pure Appl. Opt.* **8**, S278–S284 (2006).
- [132] S. Kujala, B. K. Canfield, M. Kauranen, Y. Svirko, and J. Turunen, “Multipolar analysis of second-harmonic radiation from gold nanoparticles,” *Opt. Express* **16**, 17196 (2008).
- [133] M. Zdanowicz, S. Kujala, H. Husu, and M. Kauranen, “Effective medium multipolar tensor analysis of second-harmonic generation from metal nanoparticles,” *New J. Phys.* **13**, 023025 (2011).
- [134] M. J. Huttunen, J. Mäkitalo, G. Bautista, and M. Kauranen, “Multipolar second-harmonic emission with focused Gaussian beams,” *New J. Phys.* **14**, 113005 (2012).
- [135] S. Kujala, B. K. Canfield, M. Kauranen, Y. Svirko, and J. Turunen, “Multipole interference in the second-harmonic optical radiation from gold nanoparticles,” *Phys. Rev. Lett.* **98**, 167403 (2007).
- [136] B. K. Canfield, S. Kujala, K. Laiho, K. Jefimovs, J. Turunen, and M. Kauranen, “Chirality arising from small defects in gold nanoparticle arrays,” *Opt. Express* **14**, 950 (2006).
- [137] B. K. Canfield, H. Husu, J. Laukkanen, B. Bai, M. Kuitinen, J. Turunen, and M. Kauranen, “Local field asymmetry drives second-harmonic generation in noncentrosymmetric nanodimers,” *Nano Lett.* **7**, 1251–1255 (2007).
- [138] H. Husu, B. K. Canfield, J. Laukkanen, B. Bai, M. Kuitinen, J. Turunen, and M. Kauranen, “Chiral coupling in gold nanodimers,” *Appl. Phys. Lett.* **93**, 183115 (2008).
- [139] H. Husu, R. Siikanen, J. Mäkitalo, J. Lehtolahti, J. Laukkanen, M. Kuitinen, and M. Kauranen, “Metamaterials with tailored nonlinear optical response,” *Nano Lett.* **12**, 673–677 (2012).
- [140] M. W. Klein, C. Enkrich, M. Wegener, and S. Linden, “Second-harmonic generation from magnetic metamaterials,” *Science* **313**, 502–504 (2006).
- [141] M. A. van der Veen, G. Rosolen, T. Verbiest, M. K. Vanbel, B. Maes, and B. Kolaric, “Nonlinear optical enhancement caused by a higher order multipole mode of metallic triangles,” *J. Mater. Chem. C* **3**, 1576–1581 (2015).
- [142] G. F. Walsh and L. D. Negro, “Enhanced second harmonic generation by photonic-plasmonic Fano-type coupling in nanoplasmonic arrays,” *Nano Lett.* **13**, 3111–3117 (2013).
- [143] L.-J. Black, P. R. Wiecha, Y. Wang, C. H. de Groot, V. Paillard, C. Girard, O. L. Muskens, and A. Arbouet, “Tailoring second-harmonic generation in single l-shaped plasmonic nanoantennas from the capacitive to conductive coupling regime,” *ACS Photonics* **2**, 1592–1601 (2015).
- [144] V. K. Valev, A. V. Silhanek, N. Verellen, W. Gillijns, P. V. Dorpe, O. A. Aktsipetrov, G. A. E. Vandenbosch, V. V. Moshchalkov, and T. Verbiest, “Asymmetric optical second-harmonic generation from chiral

- G-shaped gold nanostructures,” *Phys. Rev. Lett.* **104**, 127401 (2010).
- [145] V. K. Valev, X. Zheng, C. Biris, A. Silhanek, V. Volskiy, B. D. Clercq, O. A. Aktsipetrov, M. Ameloot, N. C. Panoiu, G. A. E. Vandenbosch, and V. V. Moshchalkov, “The origin of second-harmonic generation hotspots in chiral optical metamaterials,” *Opt. Mater. Expr.* **1**, 36 (2011).
- [146] V. K. Valev, J. J. Baumberg, B. D. Clercq, N. Braz, X. Zheng, E. J. Osley, S. Vandendriessche, M. Hojeij, C. Blejean, J. Mertens, C. G. Biris, V. Volskiy, M. Ameloot, Y. Ekinici, G. A. E. Vandenbosch, P. A. Warburton, V. V. Moshchalkov, N. C. Panoiu, and T. Verbiest, “Nonlinear superchiral meta-surfaces: Tuning chirality and disentangling non-reciprocity at the nanoscale,” *Adv. Mater.* **26**, 4074–4081 (2014).
- [147] K. Thyagarajan, J. Butet, and O. J. F. Martin, “Augmenting second harmonic generation using Fano resonances in plasmonic systems,” *Nano Lett.* **13**, 1847–1851 (2013).
- [148] S.-D. Liu, E. S. P. Leong, G.-C. Li, Y. Hou, J. Deng, J. H. Teng, H. C. Ong, and D. Y. Lei, “Polarization-independent multiple Fano resonances in plasmonic nonamers for multimode-matching enhanced multiband second-harmonic generation,” *ACS Nano* **10**, 1442–1453 (2016).
- [149] G. Gonella and H.-L. Dai, “Second harmonic light scattering from the surface of colloidal objects: Theory and applications,” *Langmuir* **30**, 2588–2599 (2014).
- [150] J. Butet, K. Thyagarajan, and O. J. F. Martin, “Ultra-sensitive optical shape characterization of gold nanoantennas using second harmonic generation,” *Nano Lett.* **13**, 1787–1792 (2013).
- [151] J. Butet and O. J. F. Martin, “Nonlinear plasmonic nanorulers,” *ACS Nano* **8**, 4931–4939 (2014).
- [152] S. Shen, L. Meng, Y. Zhang, J. Han, Z. Ma, S. Hu, Y. He, J. Li, B. Ren, T.-M. Shih, Z. Wang, Z. Yang, and Z. Tian, “Plasmon-enhanced second-harmonic generation nanorulers with ultrahigh sensitivities,” *Nano Lett.* **15**, 6716–6721 (2015).
- [153] H. Shen, N. Nguyen, D. Gachet, V. Maillard, T. Toury, and S. Brasselet, “Nanoscale optical properties of metal nanoparticles probed by second-harmonic generation microscopy,” *Opt. Express* **21**, 12318 (2013).
- [154] S. Kruk, M. Weismann, A. Y. Bykov, E. A. Mamonov, I. A. Kolmychek, T. Murzina, N. C. Panoiu, D. N. Neshev, and Y. S. Kivshar, “Enhanced magnetic second-harmonic generation from resonant metasurfaces,” *ACS Photonics* **2**, 1007–1012 (2015).
- [155] L. Wang, A. S. Shorokhov, P. N. Melentiev, S. Kruk, M. Decker, C. Helgert, F. Setzpfandt, A. A. Fedyanin, Y. S. Kivshar, and D. N. Neshev, “Multipolar third-harmonic generation in fishnet metamaterials,” *ACS Photonics* (2016).
- [156] I. V. Shadrivov, M. Lapine, and Y. S. Kivshar, eds., *Nonlinear, Tunable and Active Metamaterials* (Springer International Publishing, 2015).
- [157] M. Lapine, I. V. Shadrivov, and Y. S. Kivshar, “Nonlinear metamaterials,” *Reviews of Modern Physics* **86**, 1093–1123 (2014).
- [158] A. Rose, D. Huang, and D. R. Smith, “Nonlinear interference and unidirectional wave mixing in metamaterials,” *Phys. Rev. Lett.* **110**, 063901 (2013).
- [159] A. Rose, D. A. Powell, I. V. Shadrivov, D. R. Smith, and Y. S. Kivshar, “Circular dichroism of four-wave mixing in nonlinear metamaterials,” *Phys. Rev. B* **88**, 195148 (2013).
- [160] E. Poutrina and A. Urbas, “Multipolar interference for non-reciprocal nonlinear generation,” *Sci. Rep.* **6**, 25113 (2016).
- [161] E. Kim, F. Wang, W. Wu, Z. Yu, and Y. R. Shen, “Nonlinear optical spectroscopy of photonic metamaterials,” *Phys. Rev. B* **78**, 113102 (2008).
- [162] J. Reinhold, M. R. Shcherbakov, A. Chipouline, V. I. Panov, C. Helgert, T. Paul, C. Rockstuhl, F. Lederer, E.-B. Kley, A. Tünnermann, A. A. Fedyanin, and T. Pertsch, “Contribution of the magnetic resonance to the third harmonic generation from a fishnet metamaterial,” *Phys. Rev. B* **86**, 115401 (2012).
- [163] A. S. Shorokhov, K. I. Okhlopkov, J. Reinhold, C. Helgert, M. R. Shcherbakov, T. Pertsch, and A. A. Fedyanin, “Ultrafast control of third-order optical nonlinearities in fishnet metamaterials,” *Sci. Rep.* **6**, 28440 (2016).
- [164] I. A. Kolmychek, A. Y. Bykov, E. A. Mamonov, and T. V. Murzina, “Second-harmonic generation interferometry in magnetic-dipole nanostructures,” *Opt. Lett.* **40**, 3758 (2015).
- [165] R. Chandrasekar, N. K. Emani, A. Lagutchev, V. M. Shalaev, C. Ciraci, D. R. Smith, and A. V. Kildishev, “Second harmonic generation with plasmonic metasurfaces: direct comparison of electric and magnetic resonances,” *Opt. Mater. Express* **5**, 2682 (2015).
- [166] P. Albella, R. A. de la Osa, F. Moreno, and S. A. Maier, “Electric and magnetic field enhancement with ultralow heat radiation dielectric nanoantennas: Considerations for surface-enhanced spectroscopies,” *ACS Photonics* **1**, 524–529 (2014).
- [167] S. Jahani and Z. Jacob, “All-dielectric metamaterials,” *Nat. Nanotechnol.* **11**, 23–36 (2016).
- [168] A. Garcia-Etxarri, R. Gómez-Medina, L. S. Froufe-Pérez, C. López, L. Chantada, F. Scheffold, J. Aizpurua, M. Nieto-Vesperinas, and J. J. Sáenz, “Strong magnetic response of submicron silicon particles in the infrared,” *Opt. Express* **19**, 4815 (2011).
- [169] A. E. Krasnok, A. E. Miroshnichenko, P. A. Belov, and Y. S. Kivshar, “Huygens optical elements and yagi—uda nanoantennas based on dielectric nanoparticles,” *Jetp Lett.* **94**, 593–598 (2011).
- [170] A. E. Krasnok, A. E. Miroshnichenko, P. A. Belov, and Y. S. Kivshar, “All-dielectric optical nanoantennas,” *Opt. Express* **20**, 20599 (2012).
- [171] M. K. Schmidt, R. Esteban, J. J. Sáenz, I. Suárez-Lacalle, S. Mackowski, and J. Aizpurua, “Dielectric antennas - a suitable platform for controlling magnetic dipolar emission,” *Opt. Express* **20**, 13636 (2012).
- [172] M. R. Shcherbakov, D. N. Neshev, B. Hopkins, A. S. Shorokhov, I. Staude, E. V. Melik-Gaykazyan, M. Decker, A. A. Ezhov, A. E. Miroshnichenko, I. Brener, A. A. Fedyanin, and Y. S. Kivshar, “Enhanced third-harmonic generation in silicon nanoparticles driven by magnetic response,” *Nano Lett.* **14**, 6488–6492 (2014).
- [173] R. Sanatinia, S. Anand, and M. Swillo, “Modal engineering of second-harmonic generation in single GaP nanopillars,” *Nano Lett.* **14**, 5376–5381 (2014).
- [174] M. R. Shcherbakov, A. S. Shorokhov, D. N. Neshev, B. Hopkins, I. Staude, E. V. Melik-Gaykazyan,

- A. A. Ezhov, A. E. Miroshnichenko, I. Brener, A. A. Fedyanin, and Y. S. Kivshar, “Nonlinear interference and tailorable third-harmonic generation from dielectric oligomers,” *ACS Photonics* **2**, 578–582 (2015).
- [175] M. R. Shcherbakov, P. P. Vabishchevich, A. S. Shorokhov, K. E. Chong, D.-Y. Choi, I. Staude, A. E. Miroshnichenko, D. N. Neshev, A. A. Fedyanin, and Y. S. Kivshar, “Ultrafast all-optical switching with magnetic resonances in nonlinear dielectric nanostructures,” *Nano Lett.* **15**, 6985–6990 (2015).
- [176] Y. Yang, W. Wang, A. Boulesbaa, I. I. Kravchenko, D. P. Briggs, A. Puretzky, D. Geohegan, and J. Valentine, “Nonlinear Fano-resonant dielectric metasurfaces,” *Nano Lett.* **15**, 7388–7393 (2015).
- [177] L. Carletti, A. Locatelli, O. Stepanenko, G. Leo, and C. D. Angelis, “Enhanced second-harmonic generation from magnetic resonance in AlGaAs nanoantennas,” *Opt. Express* **23**, 26544 (2015).
- [178] M. Maragkou, “Dielectric nanostructures: Ultrafast responses,” *Nature Materials* **14**, 1086 (2015).
- [179] S. Makarov, S. Kudryashov, I. Mukhin, A. Mozharov, V. Milichko, A. Krasnok, and P. Belov, “Tuning of magnetic optical response in a dielectric nanoparticle by ultrafast photoexcitation of dense electron–hole plasma,” *Nano Lett.* **15**, 6187–6192 (2015).
- [180] L. Carletti, A. Locatelli, D. Neshev, and C. D. Angelis, “Shaping the radiation pattern of second-harmonic generation from AlGaAs dielectric nanoantennas,” *ACS Photonics* (2016).
- [181] P. A. Dmitriev, D. G. Baranov, V. A. Milichko, S. V. Makarov, I. S. Mukhin, A. K. Samusev, A. E. Krasnok, P. A. Belov, and Y. S. Kivshar, “Resonant Raman scattering from silicon nanoparticles enhanced by magnetic response,” *Nanoscale* **8**, 9721–9726 (2016).
- [182] A. S. Shorokhov, E. V. Melik-Gaykazyan, D. A. Smirnova, B. Hopkins, K. E. Chong, D.-Y. Choi, M. R. Shcherbakov, A. E. Miroshnichenko, D. N. Neshev, A. A. Fedyanin, and Y. S. Kivshar, “Multifold enhancement of third-harmonic generation in dielectric nanoparticles driven by magnetic Fano resonances,” *Nano Lett.* (2016).
- [183] D. G. Baranov, S. V. Makarov, V. A. Milichko, S. I. Kudryashov, A. E. Krasnok, and P. A. Belov, “Nonlinear transient dynamics of photoexcited silicon nanoantenna for ultrafast all-optical signal processing,” *arXiv:1603.04397v2* (2016).
- [184] G. Grinblat, Y. Li, M. P. Nielsen, R. F. Oulton, and S. A. Maier, “Enhanced third harmonic generation in single germanium nanodisks excited at the anapole mode,” *Nano Lett.* **16**, 4635–4640 (2016).
- [185] V. F. Gili, L. Carletti, A. Locatelli, D. Rocco, M. Finazzi, L. Ghirardini, I. Favero, C. Gomez, A. Lemaître, M. Celebrano, C. D. Angelis, and G. Leo, “Monolithic AlGaAs second-harmonic nanoantennas,” *Opt. Express* **24**, 15965 (2016).
- [186] A. B. Evlyukhin, S. M. Novikov, U. Zywietz, R. L. Eriksen, C. Reinhardt, S. I. Bozhevolnyi, and B. N. Chichkov, “Demonstration of magnetic dipole resonances of dielectric nanospheres in the visible region,” *Nano Lett.* **12**, 3749–3755 (2012).
- [187] A. I. Kuznetsov, A. E. Miroshnichenko, Y. H. Fu, J. Zhang, and B. Luk’yanchuk, “Magnetic light,” *Sci. Rep.* **2**, 492 (2012).
- [188] J. C. Ginn, I. Brener, D. W. Peters, J. R. Wendt, J. O. Stevens, P. F. Hines, L. I. Basilio, L. K. Warne, J. F. Ihlefeld, P. G. Clem, and M. B. Sinclair, “Realizing optical magnetism from dielectric metamaterials,” *Phys. Rev. Lett.* **108** (2012).
- [189] U. Zywietz, A. B. Evlyukhin, C. Reinhardt, and B. N. Chichkov, “Laser printing of silicon nanoparticles with resonant optical electric and magnetic responses,” *Nat. Commun.* **5**, 4402 (2014).
- [190] S. Liu, M. B. Sinclair, T. S. Mahony, Y. C. Jun, S. Campione, J. Ginn, D. A. Bender, J. R. Wendt, J. F. Ihlefeld, P. G. Clem, J. B. Wright, and I. Brener, “Optical magnetic mirrors without metals,” *Optica* **1**, 250 (2014).
- [191] U. Zywietz, M. K. Schmidt, A. B. Evlyukhin, C. Reinhardt, J. Aizpurua, and B. N. Chichkov, “Electromagnetic resonances of silicon nanoparticle dimers in the visible,” *ACS Photonics* **2**, 913–920 (2015).
- [192] W. K. Burns and N. Bloembergen, “Third-harmonic generation in absorbing media of cubic or isotropic symmetry,” *Phys. Rev. B* **4**, 3437–3450 (1971).
- [193] D. J. Moss, H. M. van Driel, and J. E. Sipe, “Dispersion in the anisotropy of optical third-harmonic generation in silicon,” *Opt. Lett.* **14**, 57 (1989).
- [194] D. J. Moss, E. Ghahramani, J. E. Sipe, and H. M. van Driel, “Band-structure calculation of dispersion and anisotropy in $\chi^{(3)}$ for third-harmonic generation in Si, Ge, and GaAs,” *Phys. Rev. B* **41**, 1542–1560 (1990).
- [195] A. D. Bristow, N. Rotenberg, and H. M. van Driel, “Two-photon absorption and kerr coefficients of silicon for 850–2200 nm,” *Appl. Phys. Lett.* **90**, 191104 (2007).
- [196] Q. Lin, J. Zhang, G. Piredda, R. W. Boyd, P. M. Fauchet, and G. P. Agrawal, “Dispersion of silicon nonlinearities in the near infrared region,” *Appl. Phys. Lett.* **91**, 021111 (2007).
- [197] J. Zhang, Q. Lin, G. Piredda, R. W. Boyd, G. P. Agrawal, and P. M. Fauchet, “Anisotropic nonlinear response of silicon in the near-infrared region,” *Appl. Phys. Lett.* **91**, 071113 (2007).
- [198] K. Ikeda, Y. Shen, and Y. Fainman, “Enhanced optical nonlinearity in amorphous silicon and its application to waveguide devices,” *Opt. Express* **15**, 17761 (2007).
- [199] L. Vivien and L. Pavesi, eds., *Handbook of Silicon Photonics* (Taylor & Francis, 2013).
- [200] X. Gai, D.-Y. Choi, and B. Luther-Davies, “Negligible nonlinear absorption in hydrogenated amorphous silicon at 1.55 μm for ultra-fast nonlinear signal processing,” *Opt. Express* **22**, 9948 (2014).
- [201] B. Hopkins, D. S. Filonov, A. E. Miroshnichenko, F. Monticone, A. Alù, and Y. S. Kivshar, “Interplay of magnetic responses in all-dielectric oligomers to realize magnetic Fano resonances,” *ACS Photonics* **2**, 724–729 (2015).
- [202] J. van de Groep and A. Polman, “Designing dielectric resonators on substrates: Combining magnetic and electric resonances,” *Opt. Express* **21**, 26285 (2013).
- [203] A. E. Miroshnichenko, A. B. Evlyukhin, Y. F. Yu, R. M. Bakker, A. Chipouline, A. I. Kuznetsov, B. Luk’yanchuk, B. N. Chichkov, and Y. S. Kivshar, “Nonradiating anapole modes in dielectric nanoparticles,” *Nat. Commun.* **6**, 8069 (2015).